Normal velocity freeze-out of the Richtmyer-Meshkov instability when a shock is reflected

J. G. Wouchuk and K. Nishihara
E.T.S.I. Industriales, Universidad de Castilla–La Mancha, 13071 Ciudad Real, Spain
and Institute of Laser Engineering, Osaka University, 2-6 Yamada-oka, Suita, Osaka, Japan
(Received 9 February 2004; published 13 August 2004)

It is known that for some values of the initial parameters that define the Richtmyer-Meshkov instability, the normal velocity at the contact surface vanishes asymptotically in time. This phenomenon, called freeze-out, is studied here with an exact analytic model. The instability freeze-out, already considered by previous authors [K. O. Mikaelian, Phys. Fluids **6**, 356 (1994), Y. Yang, Q. Zhang, and D. H. Sharp, Phys. Fluids **6**, 1856 (1994), and A. L. Velikovich, Phys. Fluids **8**, 1666 (1996)], is the result of a subtle interaction between the unstable surface and the corrugated shock fronts. In particular, it is seen that the transmitted shock at the contact surface plays a key role in determining the asymptotic behavior of the normal velocity at the contact surface. By properly tuning the fluids compressibilities, the density jump, and the incident shock Mach number, the value of the initial circulation deposited by the reflected and transmitted shocks at the material interface can be adjusted in such a way that the normal growth at the contact surface will vanish for large times. The conditions for this to happen are calculated exactly, by expressing the initial density ratio as a function of the other parameters of the problem: fluids compressibilities and incident shock Mach number. This is done by means of a linear theory model developed in a previous work [J. G. Wouchuk, Phys. Rev. E. **63**, 056303 (2001)]. A general and qualitative criterion to decide the conditions for freezing-out is derived, and the evolution of different cases (freeze-out and non-freeze-out) are studied with some detail. A comparison with previous works is also presented.

DOI: 10.1103/PhysRevE.70.026305 PACS number(s): 47.20.−k, 47.40.−x, 52.57.−z

I. INTRODUCTION

The Richtmyer-Meshkov (RM) instability develops whenever an incident planar shock collides with a contact surface separating two different fluids. Any small corrugation initially present at the material interface starts to grow and the fluids at both sides also develop perturbations in pressure, density, and velocity [1–8]. In this work we will only consider situations in which another shock is reflected at the contact surface [3,4]. In Fig. 1 we show the perturbed contact surface that separates two fluids. The reflected and transmitted shocks are also shown. We will consider ideal gases and shocks of arbitrary intensity. The incident shock comes from the right (fluid b) with the velocity $u_i\,\hat{x}$ in the laboratory reference frame. The fluid velocity behind the incident shock is $-v_1\,\hat{x}$. The incident shock compresses fluid "b" from its initial density ρ_{b0} to the value ρ_{b1}. It hits the interface at $t=0$. After the shock-interface collision, a reflected and trasmitted shock are formed. The reflected shock moves to the right with velocity $u_r\,\hat{x}$ in the laboratory frame. The density of the fluid compressed by the reflected shock is ρ_{bf}. The transmitted front moves to the left with velocity $-u_t\,\hat{x}$. It compresses fluid "a" from ρ_{a0} to the final value ρ_{bf}. In between, the contact surface moves to the left with velocity $-v_i\,\hat{x}$. The interface is assumed to have a sinusoidal corrugation with wavelength λ. The contact surface ripple before shock compression is assumed to be of the form $\psi_{i0}(y)=\psi_0\cos ky$, where $k=2\pi/\lambda$ is the perturbation wave number. Once the transmitted and reflected fronts start to move ahead of the interface, they generate sound, entropy, and vorticity perturbations. We will assume very small perturbation values for the different quantities, and use a linear theory description. The entropy and vorticity perturbations are frozen to the fluids elements, and therefore, they are stationary in a system of reference co-moving with the shocked material interface. The vorticity perturbations consist only of velocity fluctuations and the entropy perturbations consist only of density and temperature fluctuations [10]. On the contrary, the sound pressure and density fluctuations, travel with the speed of sound of each material and bounce between both fronts, generating at the same time an irrotational component for the

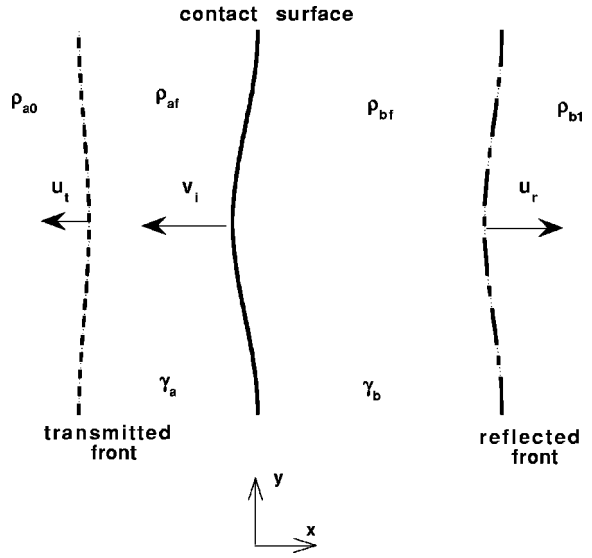

FIG. 1. Perturbed interface separating two different fluids after the interaction with an incident shock. The corrugated transmitted and reflected wave fronts are shown. For explanation of the symbols, see the text.

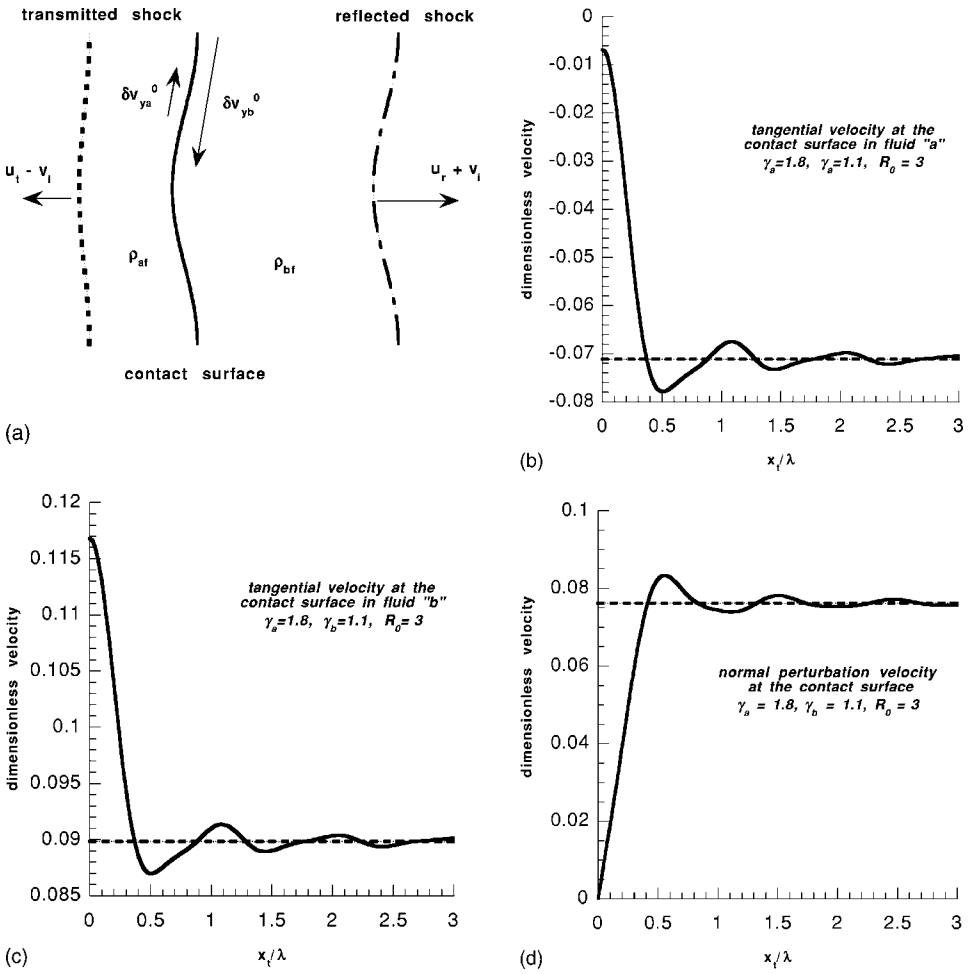

FIG. 2. (a) Normal case of the RMI, for which a positive circulation has been generated initially by the corrugated fronts at the contact surface. For details, see the text. (b) Tangential velocity on the side of fluid "*a*" for the parameters shown, as a function of dimensionless time. For details, see the text. (c) Same as (b), for the tangential velocity on side "*b*." (d) Same as (b), for the normal velocity at the contact surface.

velocity field [10]. Initially, at $t=0+$, the shocks generate tangential velocity profiles along the contact surface. On the side of fluid "*a*" the initial tangential velocity profile is $\delta v_{ya}^0 \sin ky$ and on the side of fluid "*b*" it is $\delta v_{yb}^0 \sin ky$. That is, there is an initial circulation distributed along the material interface. We define $\delta\Gamma_0 = \delta v_{yb}^0 - \delta v_{ya}^0$, which is indicated in Fig. 2(a) with the arrows corresponding to the tangential velocities. Due to the sound waves that arrive to the contact surface from both sides, this circulation will change in time, because of baroclinic effects, and arrive to an asymptotic value which we call $\delta\Gamma_\infty$ [6–9]. Meanwhile, the normal velocity is also changing in time, adjusting itself to the instantaneous value of the circulation at the interface. The interaction between the shock fronts and the interface via the sound waves that reverberate in the space in between is responsible for the temporal evolution of the perturbations in the whole flow field. Asymptotically in time, the shock fronts will regain their planar shape, the sound waves fluctuations would have almost vanished, and there will be stationary velocity, vorticity and entropy perturbation patterns at both sides of the contact interface. The asymptotic rate of growth of the ripple at the interface is determined by an adequate average of the vorticity field at each side of the material surface [7–10]. We have four dimensionless parameters that are necessary to describe the instability evolution. They are: the initial density jump $R_0 = \rho_{a0}/\rho_{b0}$, the fluids compressibilities (which for ideal gases can be described by the isentropic exponents γ_a and γ_b), and the incident shock Mach number (M_i), which determines the degree of compression suffered by both fluids. By adequately changing these four parameters we could, in principle, pass continuously from a situation in which a shock is reflected to another one in which a rarefaction is reflected, as a result of the "incident shock-interface" interaction. In this work we will only study the shock reflected situations. Typically, this amounts to considering situations in which $R_0 > 1$ for equal γ at both sides. For different values of the fluid isentropic exponents, the conditions that must be satisfied in order to have a reflected shock or rarefaction will be a definite function of R_0, M_i and γ_a, γ_b [3,4]. As is already known, whenever a shock is reflected, the asymptotic rate of growth is usually a positive quantity. This means that the interface ripple will grow without inverting its phase [1–10]. However, as has been seen in relatively recent works [3,4,9], we could also have an interface phase inversion, and still having a shock reflected, when $R_0 \sim 1$. This situation has been called "indirect phase inversion" in Ref. [3]. This means that in between, we could be able to observe a zero asymptotic rate of growth at the interface [4]. This possibility, which has been called *freeze-out* of the perturbation [11], has been predicted by Fraley in Ref. [10], and studied in some detail later by Mikaelian [11], and addressed later on by Yang, Zhang, and Sharp [3], and by Velikovich [4,11]. The possibility of observing this type of perturbation evolution was also confirmed numerically by Yang *et al.* [3],

and also with independent analytic calculations [7,9]. Fraley concluded that the situations in which freeze-out could occur should have $R_0 < 1.5$. This prediction was confirmed later on by Mikaelian, who derived an approximate expression for the growth rate, valid up to second order in $M_i^2 - 1$ (therefore, his conclusions are approximately valid for relatively weak shocks) and derived an approximate formula that locates points of freeze-out, under the assumption that the initial density ratio at the interface equals unity ($R_0 = 1$) [11]. Mikaelian also stressed the necessity of having different values for the isentropic exponents at both sides of the interface, a result that is confirmed by our calculations. However, contrary to the initial belief, there is no need to choose very different or exotic gamma values in order to find freeze-out. The only practical restriction that we have found is that the fluids should have approximately similar pre-shock mass densities. As discussed by Velikovich [4], freeze-out of the normal velocity perturbation is not a most rare occurrence. If we start with a given set of γ_a, γ_b, M_i, and $R_0 > 1$ values, such that a shock is reflected, and start decreasing the initial density ratio, we will continuously pass from the shock reflected case to the rarefaction reflected situation. Together with this change, the phase of the interface ripple will also get inverted at some intermediate density jump R_0, and the asymptotic growth rate could then be negative for $R_0 \sim 1$ [2–4]. Thus, at some specific value of the pre-shock density jump, the asymptotic growth rate equals zero [4]. It turns out to be the case that, if we start with shock reflected situations and decrease the initial parameter R_0, freeze-out conditions will cluster around $R_0 \sim 1$. To get a simple, qualitative, yet rigorous picture of the physics of freeze-out, it is better to briefly discuss two opposite cases of non-freeze-out. One in which the growth is positive and another one in which the asymptotic growth at the interface shows indirect phase inversion. After that, we analyze in a qualitative way a freeze-out situation in an effort to grasp the underlying physics.

A. Non-freeze-out cases

At first, let us consider an incident shock (Mach number $M_i = 5$) that travels inside a fluid with isentropic exponent $\gamma_b = 1.1$. The heavier fluid has $\gamma_a = 1.8$ and the initial density ratio at the contact surface is $R_0 = 3$. The transmitted and reflected shock fronts start to move away from the interface at $t = 0+$. In Fig. 2(a) we show the deformed interface, the corrugated shock fronts, and the tangential velocities around $t = 0+$. The tangential velocities have the values $\delta v_{ya}^0 \approx -0.006\,844\, u_i k \psi_0$ and $\delta v_{yb}^0 \approx 0.1168\, u_i k \psi_0$. With a linear theory model like that of Ref. [6] (previous minor errors in that reference have been corrected), the temporal evolution of the magnitudes at the interface can be studied. In Figs. 2(b) and 2(c) we show the temporal evolution of the tangential velocities at both sides of the interface. The horizontal axis is given as the distance traveled by the transmitted shock in units of the contact surface perturbation wavelength. We see that both tangential velocity perturbations arrive to a constant asymptotic value. These asymptotic values are indicated with dashed lines, and are calculated with the method described in Ref. [9]. The asymptotic values are: $\delta v_{ya}^\infty \approx -0.071\,17\, u_i k \psi_0$ and $\delta v_{yb}^\infty \approx 0.089\,98\, u_i k \psi_0$. The final interface circulation ($\delta \Gamma_\infty \approx 0.01863\, u_i k \psi_0$) has the same sign as the initial circulation ($\delta \Gamma_0 \approx 0.1236\, u_i k \psi_0$), for the parameters chosen in this case. We show next the temporal evolution of the normal velocity at the interface ripple in Fig. 2(d). It is seen that after some oscillations (the characteristic period is determined by the sound waves that reverberate at both sides of the contact surface [5,10]), the ripple attains a constant rate of growth, after the shock has moved some wavelengths away. The dashed line is the asymptotic normal velocity, also calculated with the algorithm developed in Ref. [9]. Its value is: $\delta v_i^\infty \approx 0.076\,19\, u_i k \psi_0$. As the shock considered here is quite strong, and one of the fluids is very compressible, there is some finite time before the linear asymptotic regime is achieved. Of course, for finite values of the interface ripple amplitude, the rate of growth will be later modified because of nonlinear effects, and the growth will be reduced [8,12]. Therefore, for a practical situation in which ψ_0 is not a negligible fraction of λ, the behavior shown in Fig. 2 will be of limited validity in time. Anyway, we restrict our discussion to situations in which $\psi_0 \ll \lambda$ and non-linear effects can be safely ignored.

We show in Fig. 3(a), the initial configuration of tangential velocities and shock and interface ripples, for a case in which $\gamma_a = 1.8$, $\gamma_b = 1.1$, $M_i = 5$, as before, but $R_0 = 1$. We have reduced the density jump in order to find an indirect rate of growth at the interface ripple. As can be seen from Fig. 3(a), the quantity $\delta v_{ya}^0 \approx 0.2294\, u_i k \psi_0$ has now the same sign as $\delta v_{yb}^0 \approx 0.019\,67\, u_i k \psi_0$. Furthermore, we see that it is $\delta v_{ya}^0 \gg \delta v_{yb}^0 > 0$, for this case. It is also seen that the transmitted front has inverted its phase in this situation, as compared to the case discussed above. The initial circulation ($\delta \Gamma_0 \approx -0.2098\, u_i k \psi_0$) has changed sign with respect to the case discussed before. In Figs. 3(b) and 3(c) we show the temporal evolution of the tangential velocities at the interface. The asymptotic values of the contact surface tangential velocities are: $\delta v_{ya}^\infty \approx 0.096\,72\, u_i k \psi_0$ and $\delta v_{yb}^\infty \approx -0.011\,15\, u_i k \psi_0$, which give $\delta \Gamma_\infty \approx -0.1079\, u_i k \psi_0$. The normal perturbation velocity at the interface is shown in Fig. 3(d). The asymptotic value is $\delta v_i^\infty \approx -0.011\,36\, u_i k \psi_0$. It is clear that the phase of the contact surface corrugation has changed sign early during perturbation growth and therefore, the final asymptotic growth proceeds in the opposite direction as compared to the previous case. Where is the reason for this anomalous behavior? It is impossible to give in simple mathematical terms a simple algebraic condition to be fulfilled, in such a way that the anomalous phase inversion could be easily predicted. This is so, because it is the result of a subtle interaction between the interface perturbations and the sound pressure fluctuations coming from the shocks at each side of the contact surface. The interaction between interface and shock perturbations is of non-local nature in time, a fact which unfortunately complicates the mathematical description in simpler terms. Even more so, if the sound speeds at both sides are different, because the fluid with lesser sound speed will arrive much later to the asymptotic stage and hence, we have a mismatch of signals at the contact surface [10]. These effects are a consequence of the fluids compressibilities, as already recognized by previous authors [4,5,10,11]. We can get, however,

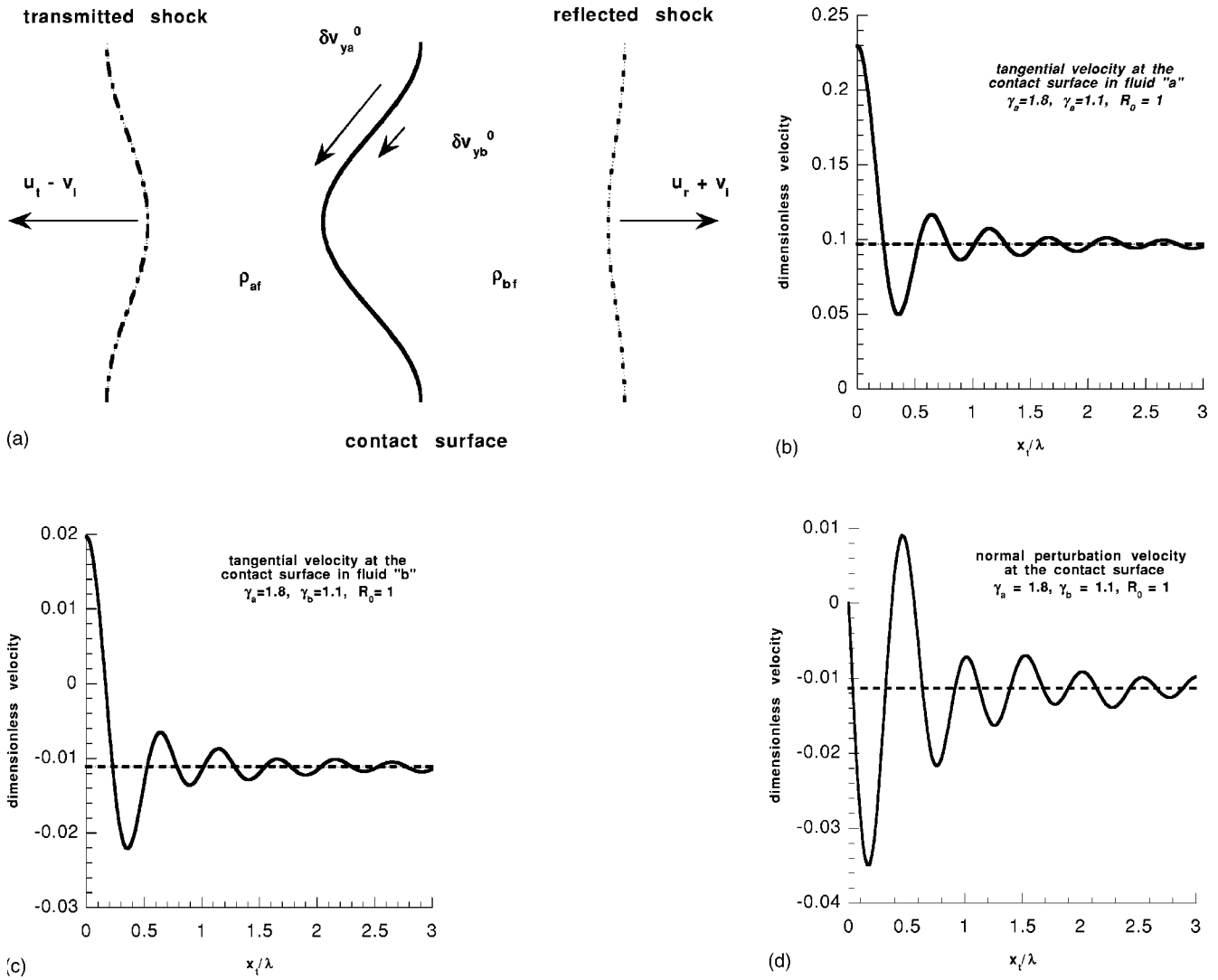

FIG. 3. (a) Same as 2(a), but for a case in which the initial circulation is negative. For details, see the text. (b) Tangential velocity on the side of fluid "*a*" for the parameters shown, as a function of dimensionless time. For details, see the text. (c) Same as (b), for the tangential velocity on side "*b*." (d) Same as (b), for the normal velocity at the contact surface.

a qualitative understanding of the indirect phase inversion, by looking at the initial tangential velocities. In fact, the initial ripples of the reflected and transmitted shock fronts are given by [1,3–5,10]

$$\psi_{r0} = \left(1 + \frac{u_r}{u_i}\right)\psi_0, \tag{1}$$

$$\psi_{t0} = \left(1 - \frac{u_t}{u_i}\right)\psi_0, \tag{2}$$

from which the initial tangential velocities behind the corrugated fronts can be calculated [1,3,4]:

$$\delta v_{yb}^0 = (v_1 - v_i)\psi_{r0}, \tag{3}$$

$$\delta v_{ya}^0 = -v_i\psi_{t0}. \tag{4}$$

In a case like the one studied in Fig. 2, the fluids and shock parameters are such that $u_t < u_i$. In fact, we get $u_t/u_i \approx 0.9901 < 1$. This means that the initial circulation is positive ($\delta\Gamma_0 > 0$). The subsequent interaction with the sound waves does not modify the sign of this circulation and therefore, the interface ripple does not change phase.

Let us now consider the case studied in Fig. 3. For the parameters of this situation, we get $u_t/u_i \approx 1.2648 > 1$. This means that the transmitted shock front ripple has an inverted phase with respect to the initial interface corrugation (at $t = 0+$). Then, the initial tangential velocity induced by the transmitted front has the same sign as the tangential velocity behind the reflected shock. Furthermore, the absolute values are such that the tangential velocity on side "*a*" is "stronger" than that on side "*b*". That is, the initial circulation is now negative ($\delta\Gamma_0 < 0$). The following interaction of this circulation with the pressure gradient induced by the incoming sound waves (for $t > 0$) will make the final circulation remain negative, in such a way that a negative normal growth is observed at the interface ripple. The natural question is then, how much faster should the transmitted shock move com-

pared to the incident shock, in order to stop the growth at the interface, asymptotically in time. Two points are noted: first, the requirement $u_t = u_i$ will not give freeze-out, because $\delta\Gamma_0 > 0$ and the interaction with the sound waves does not seem to be strong enough to reduce the growth to zero in this case. Second, the cases in which $\delta v_{ya}^0 = \delta v_{yb}^0$ would also not conduct us to a freeze-out case, because, even if $\delta\Gamma_0 = 0$, its value will not remain zero because of the baroclinic interaction with the pressure field of the sound waves. The exact amount by which u_t should exceed u_i in order to have freeze-out is determined by the interaction between the perturbations at the contact surface and those which are generated at the corrugated shock fronts [5,10]. In other words, there should be a definite value for the ratio $K_0 = \delta v_{ya}^0 / \delta v_{yb}^0$, such that if the parameter K_0 equals some critical value K_0^{fo}, then freeze-out results. For values of K_0 different from K_0^{fo}, positive or negative growth would be the outcome. A quantitative determination of K_0^{fo}, in order to decide whether freeze-out will occur or not, is far from being simply written in terms of the initial parameters that describe the zero order flow.

B. Freeze-out situation

We discuss now a situation which is almost near freeze-out conditions. Strictly speaking, to start the discussion in more precise terms, the freeze-out conditions should be sought by requiring the vanishing of the asymptotic normal velocity perturbation at the interface. To be successful, we must use an exact expression for the asymptotic rate of growth. To this scope, it is very convenient to use the exact formula derived in Refs. [7,9]:

$$\delta v_i^{\infty} = \frac{\delta v_{yb}^0 - R\,\delta v_{ya}^0}{R+1} + \frac{RF_a - F_b}{R+1} = 0, \tag{5}$$

where δv_i^{∞} is the asymptotic normal velocity at the interface ripple, $R = \rho_{af}/\rho_{bf}$ is the final density ratio at the contact surface, and $F_{a,b}$ represent the interaction of the corrugated interface with the sound waves emitted by the deformed shock fronts. It is also seen that the quantities $F_{a,b}$ can be thought of as representing a weighted spatial average of the vorticity perturbation field left by the corrugated fronts in the bulk of the fluids [7,9]. In this sense, we also speak of them as representing the asymptotic effect of the bulk vorticities on the interface asymptotic evolution. For a completely irrotational problem (which never occurs with corrugated shocks), the quantities $F_{a,b}$ would be exactly equal to zero. This situation is never realized in practice, for shock reflected cases. It can be used as an approximation for very weak shocks. Indeed, as has already been shown in Refs. [7,9], the bulk vorticity factors $F_{a,b}$ are proportional to $(M_i^2-1)^3$ for very weak shocks. This result would induce us to think that for very weak shocks, freezing-out conditions could be derived by requiring the vanishing of just the irrotational contribution of Eq. (5). As will be seen later, this is not strictly correct and could be misleading, even for weak shocks. This means that to correctly understand the peculiar phenomenon of asymptotic freeze-out, we must include the terms that result from the shocks-interface interaction. In the following sections, we will develop the algorithm that allows us to find the solution to Eq. (5). To make a qualitative introduction here, we have chosen the same values of M_i, γ_a, and γ_b as before, and leave R_0 undetermined. When Eq. (5) is solved with the method explained later, we get $R_0 \approx 1.157\,927\,1\ldots$. For this precision in the density jump, the perturbation normal velocity at the interface satisfies $\delta v_i^{\infty} < 10^{-10}$ in units of $u_i k \psi_0$. Obviously, if we continued calculating more digits for R_0, we would have obtained lower and lower bounds for the perturbation velocity, approaching the zero value for the correct combination of infinite digits in R_0. For the purpose of the discussion here, it is enough to set δv_i^{∞} less than a low enough value. In Fig. 4(a) we show the initial tangential velocities at the interface and the corrugated shocks, where the phase inversion of the transmitted front has been evidenced. In Figs. 4(b) and 4(c), we show the tangential velocities evolution as a function of the distance traveled by the transmitted shock. In Fig. 4(d) we show the evolution of the normal velocity perturbation at the interface ripple. For the case discussed here, the initial tangential velocities on both sides of the interface are given by $\delta v_{ya}^0 \approx 0.1906\, u_i k \psi_0$ and $\delta v_{yb}^0 \approx 0.0303$. Later on, they are modified because of the baroclinic interaction with the sound pressure field, and we get the asymptotic tangential velocities $\delta v_{ya}^{\infty} \approx 0.0722\, u_i k \psi_0$ and $\delta v_{yb}^{\infty} \approx 0.000\,643\,7\, u_i k \psi_0$. This makes a negative asymptotic circulation: $\delta\Gamma_{\infty} \approx -0.0716\, u_i k \psi_0 \neq 0$, but zero asymptotic normal velocity. There is no contradiction in this result, as there is a vorticity field at both sides of the interface, which is responsible for generating finite tangential velocities at the contact surface. This means that, despite the fact the interface ripple does not grow normally, the bulk of the fluids show persistent and steady asymptotic velocity perturbations, which are rotational in nature, as they are that part of the velocity field which was generated by the corrugated shock fronts. For example, in the general case, the normal velocity fluctuations behind the shock front can always be decomposed in the form [10]:

$$\delta v_x(x,y,t) = \delta v_x^{(\mathrm{pot})}(x,y,t) + \delta v_x^{(\mathrm{rot})}(x,y), \tag{6}$$

where $\delta v_x^{(\mathrm{pot})}$ is the irrotational contribution to the velocity field due to the pressure generated by the reverberating sound waves. This part of the velocity field does change in time, but gives no contribution to vorticity, as it is an irrotational mode [4,10]. On the other hand, the second part, given by $\delta v_x^{(\mathrm{rot})}$, is a steady state contribution (in a system of reference co-moving with the shocked contact surface), which does not change in time. Furthermore, it is always $\delta v_x^{(\mathrm{rot})}(x=0)=0$. That is, the rotational part of the velocity field always vanishes at the contact surface ripple, independently of the properties of the fluids or the shock intensity, because the initial $(t=0+)$ pressure fluctuations between the corrugated shock fronts are zero [1,3,7,9,10]. Therefore, the asymptotic velocity at the interface is the result of making $t \to \infty$ and $x=0$ in the above equation. The freeze-out situations would correspond to cases in which $\delta v_x^{(\mathrm{pot})}(x=0, y, t\to\infty)=0$, which also implies that $\delta v_x^{(\mathrm{pot})}(x\neq 0, y, t\to\infty)=0$, because this a potential contribution (it is always irrotational and becomes a divergence free field, asymptotically in time, because the

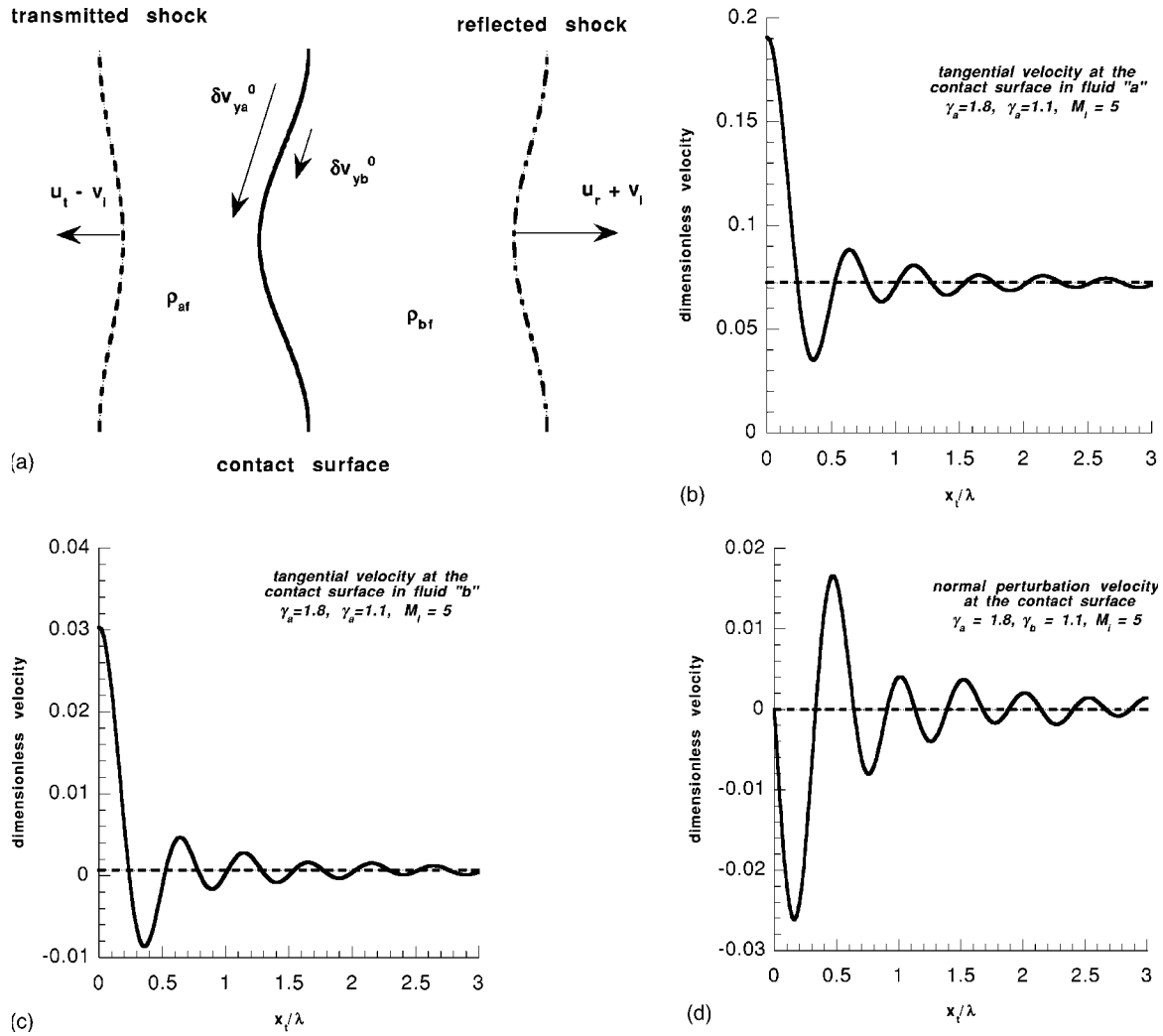

FIG. 4. (a) Same as 3(a), but for a case which shows asymptotic freeze-out. (b) Tangential velocity on the side of fluid "*a*" for the parameters shown, as a function of dimensionless time. For details, see the text. (c) Same as (b), for the tangential velocity on side "*b*." (d) Same as (b), for the normal velocity at the contact surface.

density perturbations do not change in time, at large times). However, as the vorticity is a conserved quantity for inviscid fluids, it is clear that even in freeze-out conditions, the second [rotational contribution $\delta v_x^{(\mathrm{rot})}$, in Eq. (6)], will remain different from zero for $x \neq 0$, and equal to the value generated by the corresponding fronts. This means that the fluids would keep "revolving" at each side of the interface. In this form, the fluids keep memory of the fact that the shock fronts were corrugated when they separated from each other, and that they compressed non-uniformly the different fluid elements, generating steady entropy and vorticity fluctuations along their way. In consequence, we could never speak of a proper "stabilization" of the perturbation field, because some energy will still remain in the fluids as rotational motion. The effect of these perturbations would not be manifested as motion in the normal direction, but rather in the form of vortices that persist indefinitely in time. It is only the normal velocity at the interface that vanishes (asymptotically in time). On the contrary, this does not happen to the normal and tangential velocities in the bulk of the fluids. Of course, the absolute values of those magnitudes inside the fluids would be surely smaller in a freeze-out case as compared to a non-freeze-out case, but this would require a specific evaluation case by case. This persistency of the perturbations inside the fluids could also have deleterious effects, for example in inertial confinement fusion (ICF), if another shock is launched after the first one (assuming that the first shock has frozen out the perturbation growth at the interface). It is clear that a deeper understanding of freeze-out in the RM instability would be helpful not only because of its potential application in fields like ICF, but also because it will help to gain a better understanding of the role of compressibility in general instability evolution. To properly discuss these issues, we have organized this work as follows: in Sec. II, the basic equations for the zero order flow and the perturbed quantities are presented. In Sec. III the method to determine the freeze-out conditions is explained. The results of these calculations are also shown in Sec. III. A discussion is presented in Sec. IV and the results obtained here are compared with those found in previous works. A brief summary is presented in Sec. V.

II. BASIC EQUATIONS

In this section we define the basic magnitudes of the zero order flow and the equations satisfied by the perturbed quantities. They are the necessary ingredients before the derivation of the freezing-out conditions is attempted.

A. Zero order quantities

Referring to Fig. 1, and solving for the Rankine-Hugoniot equations at the shock fronts [13–15], it is easy to derive the different magnitudes of interest in the compressed fluids. We previously define the shock intensities, following Whitham [15]. In fact, let p_0 be the initial pressure of both fluids, before shock compression. If the pressure driving the incident shock is p_1, we define the incident shock intensity as $z_i=(p_1-p_0)/p_0$. It is easy to see that the incident shock Mach number is related to the shock intensity by: $z_i=2\gamma_b(M_i^2-1)/(\gamma_b+1)$. The incident shock speed in the laboratory frame is therefore:

$$u_i = c_{b0}\sqrt{1+\left(\frac{\gamma_b+1}{2\gamma_b}\right)z_i}. \tag{7}$$

Besides, it is not difficult to deduce the different quantities behind the front (a subscript "1" indicates the magnitudes behind the incident shock):

$$\frac{\rho_{b1}}{\rho_{b0}} = \frac{1+\epsilon_{b1}z_i}{1+\epsilon_{b2}z_i}, \tag{8}$$

$$\frac{c_{b1}}{c_{b0}} = \sqrt{(1+z_i)\frac{\rho_{b0}}{\rho_{b1}}}, \tag{9}$$

where $\epsilon_{b1,2}=(\gamma_b\pm1)/2\gamma_b$. The same magnitudes can be calculated for the flow behind the reflected and transmitted shocks. It is necessary, then, to define the reflected and transmitted shock intensities. Let p_f be the pressure between the reflected and transmitted fronts. The reflected shock intensity is: $z_r=(p_f-p_1)/p_1$, and the transmitted shock intensity is calculated with: $z_t=(p_f-p_0)/p_0$. It is not difficult to see, because of continuity of normal velocity and pressure at the contact surface, that z_r and z_t can be calculated once we specify z_i, γ_a, γ_b, and the initial density jump $R_0=\rho_{a0}/\rho_{b0}$. The two necessary equations are

$$\frac{z_i}{\sqrt{1+\epsilon_{b1}z_i}} - z_r\sqrt{\frac{(1+z_i)}{(1+\epsilon_{b1}z_r)}\frac{\rho_{b0}}{\rho_{b1}}} = \sqrt{\frac{\gamma_b}{\gamma_a R_0}}\frac{z_t}{\sqrt{1+\epsilon_{a1}}}, \tag{10}$$

$$z_t = z_i + (1+z_i)z_r, \tag{11}$$

where $\epsilon_{a1,2}=(\gamma_a\pm1)/2\gamma_a$. The flow velocity behind the reflected shock, in a system fixed to the reflected front is given by

$$v_1 - v_i = c_{b1}\frac{z_r}{\gamma_b\sqrt{1+\epsilon_{b1}z_r}}, \tag{12}$$

and the compression ratio is

$$\frac{\rho_{bf}}{\rho_{b1}} = \frac{1+\epsilon_{b1}z_r}{1+\epsilon_{b2}z_r}. \tag{13}$$

The sound speed behind the reflected shock can be calculated with

$$\frac{c_{bf}}{c_{b1}} = \sqrt{(1+z_r)\frac{\rho_{b1}}{\rho_{bf}}}. \tag{14}$$

The reflected shock speed in the laboratory reference frame is

$$u_r = c_{b1}\sqrt{1+\epsilon_{b1}z_r}. \tag{15}$$

Analogously, the density compression across the transmitted front is

$$\frac{\rho_{af}}{\rho_{a0}} = \frac{1+\epsilon_{a1}z_t}{1+\epsilon_{a2}z_t}. \tag{16}$$

The compressed sound speed is

$$\frac{c_{af}}{c_{a0}} = \sqrt{(1+z_t)\frac{\rho_{a0}}{\rho_{af}}}, \tag{17}$$

and the transmitted shock speed in the laboratory frame is

$$u_t = c_{a0}\sqrt{1+\epsilon_{a1}z_t}. \tag{18}$$

The contact surface velocity is

$$v_i = c_{a0}\frac{z_t}{\gamma_a\sqrt{1+\epsilon_{a1}z_t}}. \tag{19}$$

It is not difficult to construct the final density ratio and the ratio of compressed sound speeds at the interface:

$$R = \frac{\rho_{af}}{\rho_{bf}} = \frac{\rho_{af}}{\rho_{a0}}\frac{\rho_{b0}}{\rho_{b1}}\frac{\rho_{b1}}{\rho_{bf}}R_0, \tag{20}$$

$$N = \frac{c_{af}}{c_{bf}} = \frac{c_{af}}{c_{a0}}\frac{c_{b0}}{c_{b1}}\frac{c_{b1}}{c_{bf}}N_0, \tag{21}$$

where $N_0=c_{a0}/c_{b0}=\sqrt{\gamma_b/(\gamma_a R_0)}$ is the ratio of the pre-shock sound speeds at the interface.

B. Perturbation equations

In this section we will briefly review the equations that govern the perturbed flow between the reflected and transmitted fronts. We follow essentially the calculations shown in previous works [7,9]. The velocity, pressure, density, and entropy are assumed to satisfy the usual conservation laws in the space between the contact surface and the shocks:

$$\frac{\partial\rho}{\partial t} = -\vec{\nabla}\cdot(\rho\vec{v}), \tag{22}$$

$$\frac{\partial\vec{v}}{\partial t} + (\vec{v}\cdot\vec{\nabla})\vec{v} = -\frac{1}{\rho}\vec{\nabla}p, \tag{23}$$

$$\frac{\partial s}{\partial t} + (\vec{v}\,.\,\vec{\nabla})s = 0, \tag{24}$$

which express the conservation of mass, momentum, and entropy, respectively. We linearize the flow equations, assuming that each quantity ϕ can be decomposed as $\phi_0 + \delta\phi$, where ϕ_0 is the unperturbed (zero order) value, calculated in the previous section, and $\delta\phi$ is the small fluctuation generated because the wave fronts are corrugated. We will always assume that $\delta\phi \ll \phi_0$. We assume that the corrugated interface has the dependence $\cos ky$, and it is not difficult to see that the pressure perturbations will also depend on the tangential coordinate like $\cos ky$. Besides, the velocity components satisfy: $\delta v_x \sim \cos ky$ and $\delta v_y \sim \sin ky$. It is convenient to work with dimensionless perturbed quantities. We define (the subindex "m" refers either to "a" or "b"):

$$\delta p_m(x,y,t) = \rho_{mf} c_{mf} u_i (k\psi_0)\, \delta\hat{p}_m(x,t)\cos ky, \tag{25}$$

$$\delta v_{xm}(x,y,t) = u_i (k\psi_0)\, \delta u_m(x,t)\cos ky, \tag{26}$$

$$\delta v_{ym}(x,y,t) = u_i (k\psi_0)\, \delta v_m(x,t)\sin ky. \tag{27}$$

$$\delta \rho_m(x,y,t) = u_i (k\psi_0)\, \delta\hat{\rho}_m(x,t)\cos ky. \tag{28}$$

Thanks to the entropy conservation along the fluid particles path [Eq. (24) above], the density perturbations are related to the pressure perturbations by

$$\frac{\partial \delta p}{\partial t} = c_{mf}^2 \frac{\partial \delta\rho}{\partial t}. \tag{29}$$

On the other hand, it is easy to derive the expression for the vorticity perturbations:

$$\delta\omega_m(x,y) = \frac{\partial \delta v_{ym}(x,y,t)}{\partial x} - \frac{\partial \delta v_{xm}(x,y,t)}{\partial y} = \left[\frac{\partial \delta v_m(x,t)}{\partial x} + k\,\delta u_m(x,t) \right] \sin ky \equiv g_m(x)\sin ky. \tag{30}$$

After linearizing the equations of motion, we obtain the following wave equations for the perturbations in pressure and velocity (we omit the subscript "m" for simplicity):

$$\frac{\partial^2 \delta\hat{p}}{\partial (kc_f t)^2} - \frac{\partial^2 \hat{p}}{\partial (kx)^2} + \delta\hat{p} = 0, \tag{31}$$

$$\frac{\partial^2 \delta u}{\partial (kc_f t)^2} - \frac{\partial^2 \delta u}{\partial (kx)^2} + \delta u = g(x), \tag{32}$$

$$\frac{\partial^2 \delta v}{\partial (kc_f t)^2} - \frac{\partial^2 \delta v}{\partial (kx)^2} + \delta v = -\frac{dg(x)}{dx}. \tag{33}$$

It has been shown in previous works that the wave equation for the pressure perturbations can be easily solved by making a variable change, suggested by Zaidel' [6,7,9,16]:

$$kx = r_m \sinh\theta_m,$$

$$kc_{mf}t = r_m \cosh\theta_m. \tag{34}$$

In this new system of coordinates, the interface has the coordinate $\theta = 0$. The shock fronts, which move in the x,t variables, are now fixed in the new coordinates. That is, the reflected shock coordinate is given by: $\tanh\theta_r = \beta_r = (u_r + v_i)/c_{bf}$, where $u_r + v_i$ is the velocity of the reflected shock relative to the moving contact surface. Therefore, β_r is the reflected shock Mach number with respect to the compressed fluid "b". Analogously, the transmitted shock moves in the negative direction with velocity $-u_t\,\hat{x}$ which makes the transmitted shock coordinate in the new system to be given by: $\tanh\theta_t = -\beta_t = -(u_t - v_i)/c_{af} < 0$. The quantity $u_t - v_i$ is the transmitted shock speed relative to the material interface. The quantity β_t is the transmitted shock Mach number with respect to the fluid between the transmitted shock and contact surface.

The wave equation for the pressure perturbations in both fluids can be rewritten in the following form:

$$r_m^2 \frac{\partial^2 \delta\hat{p}_m}{\partial r_m^2} + \frac{\partial \delta\hat{p}_m}{\partial r_m} + r_m \delta\hat{p}_m = \frac{\partial \delta l_m}{\partial \theta_m}, \tag{35}$$

where the auxiliary function δl_m is given by

$$\delta l_m = \frac{1}{r_m}\frac{\partial \delta\hat{p}_m}{\delta\theta_m}. \tag{36}$$

To get the exact solution of the wave equation, it is better to work with the Laplace transform of the perturbed quantities, as suggested by Zaidel' [16]. We define Laplace transforms in the variable r_m with capital letters, for any perturbed quantity $\delta\phi_m$, as

$$\delta\Phi_m(\theta_m, s_m) = \int_0^\infty \delta\phi_m(r_m, s_m) e^{-s_m r_m} dr_m. \tag{37}$$

Laplace transforming the wave equation [Eqs. (35) and (36)], we deduce, after some long algebra [9], that the Laplace function of the pressure perturbations can be cast in a very useful form. We further define $s_m = \sinh q_m$, and obtain

$$\delta P_m(\theta_m, s_m) = \frac{F_{m1}(q_m - \theta_m) + F_{m2}(q_m + \theta_m)}{\cosh q_m}. \tag{38}$$

The Laplace transform of the pressure derivative δl_m can be written in the form:

$$\delta L_m(\theta_m, s_m) = F_{m1}(q_m - \theta_m) - F_{m2}(q_m + \theta_m). \tag{39}$$

The functions $F_{m1,2}$ have yet to be determined from the boundary conditions at the shock fronts and at the contact surface. As for their physical meaning, it can be shown, by means of the model developed by Fraley [10], that the function F_{m1} stands for the sound waves that leave the shock surface toward the interface. The function F_{m2} represents the sound waves that travel from the contact surface toward the corresponding shock front. We also note that the arguments of these functions are displaced in $\pm\theta$. This characteristic is a consequence of two facts: at first, there is a material surface that reflects the waves toward the shocks, that is, the contact surface itself, and second, we will always have the Doppler

shift at the fronts, as they are moving with a finite velocity in the frame of reference fixed to the material interface [10]. It is clear to foresee that these terms are of the utmost importance if we want to understand the instability evolution. This is so, because they are the mathematical structures responsible for describing the interaction between the fronts and the material surface. To neglect the shifts inside them would be equivalent to erasing from the problem the nicest characteristic of this instability: the sonic interaction that exists between fronts and contact surface since $t=0+$. In fact, not taking the shifts into account could be only justified when the shocks are very, very weak, because in that case, the fronts separate almost immediately from the unstable interface. They would travel at almost the speed of sound and, thus, shocks and interface decouple very soon. The perturbations emitted from the interface would take too long to arrive to the shocks and come back to the interface to repeat the process. However, this is no longer true for shocks of finite intensity. The possibility of having freeze-out at the interface, as discussed in Sec. I, comes from the fact that $F_{m1,2}(q\pm\theta)$ are important and they are not negligible in the general case. They are not only necessary to follow the sonic interaction, but also to describe the vorticity generation in the bulk. The details of the interaction between shocks and interface, which would help to explain the asymptotic freeze-out at the contact surface, are unfortunately hidden in the cumbersome mathematical structure of $F_{m1,2}$. In the following sections we will learn how to deal with them and obtain the desired conditions for freeze-out.

C. Boundary conditions

It is convenient to briefly review the boundary conditions at the shock fronts and at the material interface. This will allow us to construct the reverberating sound wave functions $F_{m1,2}$ and solve the perturbation problem. In the next section, these results will be used to determine the exact conditions that must be satisfied to have perturbation freeze-out at the contact surface.

1. Boundary conditions at the reflected shock front

Following Richtmyer [1], it is possible to arrive at an equation that involves the partial derivatives of the pressure with respect to time and normal coordinate, at each shock front. We will not repeat those calculations here, but merely write the final results, as they will be useful for the discussion that follows. After expressing that equation in the coordinates r,θ and taking its Laplace transform, we arrive at an equation that relates the perturbed quantities at the shock: $\delta P_r(s)$ and $\delta L_r(s)$. We omit the subscript "b" in the variable q_b in this paragraph, and indicate the functions pertaining to the reflected shock with a subscript "r." The boundary condition at the shock front can be put in the following form:

$$\delta L_r(q) = \alpha_{b1}(q)\,\delta P_r(q) + \alpha_{b2}(q), \tag{40}$$

where $\delta P_r(q) \equiv \delta P_b(\theta_r, \sinh q_b)$ and analogously with δL_r:

$$\alpha_{b1}(q) = \alpha_{b10}\sinh q + \frac{\alpha_{b11}}{\sinh q}. \tag{41}$$

The quantities α_{b10} and α_{b11} are given by

$$\alpha_{b10} = \frac{h_r - 1}{2\beta_r}, \tag{42}$$

$$\alpha_{b11} = -\frac{\beta_r}{1-\beta_r^2}\frac{h_r+1}{2}\frac{\rho_{bf}}{\rho_{b1}}, \tag{43}$$

where the parameter h_r is [13]

$$h_r = \frac{p_f - p_1}{V_{b1} - V_{bf}}\left(\frac{dV}{dp}\right)_{\mathrm{RH}}, \tag{44}$$

the derivative is taken along the reflected shock Rankine-Hugoniot curve in the final state, $V=1/\rho$ is the specific volume.

The function $\alpha_{b2}(q)$ is

$$\alpha_{b2}(q) = -\,\delta v_{yb}^0 \frac{\sinh\theta_r}{\sinh q}, \tag{45}$$

where δv_{yb}^0 is the initial tangential velocity behind the reflected front, defined in Eq. (3). The boundary condition written in Eq. (40) can be recast in terms of the functions $F_{b1,2}$ by means of Eqs. (38) and (39). After some algebra, we arrive at

$$F_{b1}(q) = \frac{\delta v_{yb}^0 \sinh\theta_r}{\sinh(q+\theta_r)\,\eta_r^-(q+\theta_r)} - \frac{\eta_r^+(q+\theta_r)}{\eta_r^-(q+\theta_r)}F_{b2}(q+2\theta_r), \tag{46}$$

where we have used the functions $\eta_r^{\pm}$ defined by

$$\eta_r^{\pm}(q) = \frac{\alpha_{b1}(q)}{\cosh q} \pm 1. \tag{47}$$

2. Boundary conditions at the transmitted shock front

We can manage the boundary conditions at the transmitted front in the same way as has been done with the reflected shock. We get the following corresponding equation (we do not append the subscript "a" to the variable q in this paragraph, to simplify the notation):

$$\delta L_t(q) = \alpha_{a1}(q)\,\delta P_t(q) + \alpha_{a2}(q). \tag{48}$$

We have defined $\delta P_t \equiv \delta P_a(\theta_t, \sinh q)$ and similarly with δL_t. The auxiliary function α_{a1} is

$$\alpha_{a1}(q) = \alpha_{a10}\sinh q + \frac{\alpha_{a11}}{\sinh q}, \tag{49}$$

where the quantities α_{a10} and α_{a11} are

$$\alpha_{a10} = \frac{h_t - 1}{2\beta_t}, \tag{50}$$

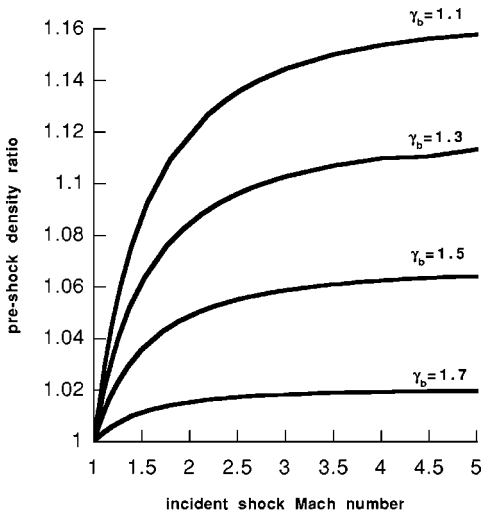

FIG. 5. Curves of freeze-out for the parameters shown. The isentropic exponent of fluid "*a*" is always $\gamma_a=1.8$.

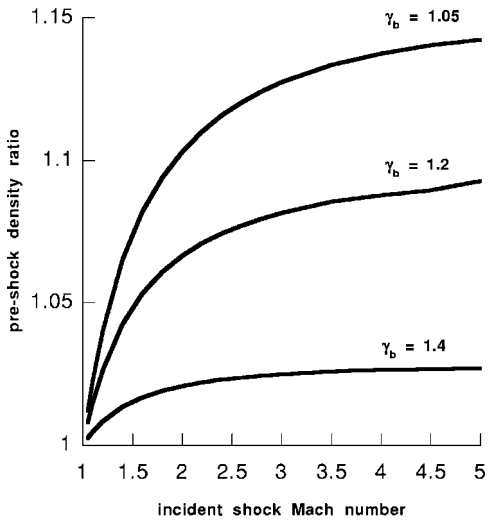

FIG. 6. Same as Fig. 5, but for $\gamma_a=1.5$.

$$\alpha_{a11}=\frac{\beta_t}{1-\beta_t^2}\frac{h_t+1}{2}\frac{\rho_{af}}{\rho_{a0}}, \tag{51}$$

with h_t a parameter defined at the transmitted shock Rankine-Hugoniot curve [13]:

$$h_t=\frac{p_f-p_0}{V_{a0}-V_{af}}\left(\frac{dV}{dp}\right)_{\mathrm{RH}}. \tag{52}$$

The function $\alpha_{a2}(q)$ is

$$\alpha_{a2}(q)=-\delta v_{ya}^0\frac{\sinh\theta_t}{\sinh q}. \tag{53}$$

Similarly, as we have done with the reflected front, we can recast the transmitted shock boundary condition in terms of $F_{a1,2}$:

$$F_{a2}(q)=\frac{\delta v_{ya}^0\sinh\theta_t}{\sinh(q-\theta_t)\eta_t^+(q-\theta_t)}-\frac{\eta_t^-(q-\theta_t)}{\eta_t^+(q-\theta_t)}F_{a1}(q-2\theta_t), \tag{54}$$

where the auxiliary functions $\eta_t^{\pm}(q)$ are given by

$$\eta_t^{\pm}(q)=\frac{\alpha_{a1}(q)}{\cosh q}\pm 1. \tag{55}$$

Up to now, we have arrived at two equations [Eqs. (46) and (54)] that relate four unknown functions [$F_{a1,2}(q_a)$ and $F_{b1,2}(q_b)$]. We need two additional equations to close the problem. Furthermore, it is noted that the variables q are different on each side of the contact surface. The task of finding the additional pair of equations and the relation between q_a and q_b is left for the next paragraph, when we look at the boundary conditions at the material interface.

3. Boundary conditions at the contact surface

At the boundary that separates both fluids, we require, as usual, the continuity of pressure and normal acceleration perturbations [1,3,4],

$$RN\delta\hat{p}_a(x=0,t)=\delta\hat{p}_b(x=0,t), \tag{56}$$

$$\frac{\partial\delta\hat{p}_a}{\partial x}=\frac{\partial\delta\hat{p}_b}{\partial x}. \tag{57}$$

To get useful relationships in terms of the functions F, it is convenient to change variables from x,t to r,θ on each fluid, separately. Besides, we note that $r_a(x=0)=kc_{af}t\equiv\tau_a$ and $r_b(x=0)=kc_{bf}t\equiv\tau_b$. If we further make a Laplace transform of Eqs. (56) and (57), we must keep in mind that the Laplace variables $s_a=\sinh q_a$, and $s_b=\sinh q_b$, at each side of the interface should be related by $s_akc_{af}t=s_bkc_{bf}t$. That is, $Ns_a=s_b$. After some algebra, and using Eqs. (38) and (39) evaluated at $x=\theta=0$, we arrive at the following relationships:

$$F_{a2}(q_a)=\frac{2F_{b2}(q_b)-(\Delta-1)F_{a1}(q_a)}{\Delta+1}, \tag{58}$$

$$F_{b1}(q_b)=\frac{2\Delta F_{a1}(q_a)+(\Delta-1)F_{b2}(q_b)}{\Delta+1}, \tag{59}$$

where $\Delta=R\cosh q_b/\cosh q_a$.

Furthermore, Eqs. (46), (54), (58), and (59) can be reduced to the system:

$$\phi_{a3}F_{a1}(q_a)+F_{b2}(q_b)=\phi_{a1}+\phi_{a2}F_{a1}(q_a-2\theta_t), \tag{60}$$

$$F_{a1}(q_a)+\phi_{b3}F_{b2}(q_b)=\phi_{b1}+\phi_{b2}F_{b2}(q_b+2\theta_r). \tag{61}$$

The auxiliary functions $\phi_{m1,2,3}$ are defined by

$$\phi_{a1}=\frac{\Delta+1}{2}\frac{\delta v_{ya}^0\sinh\theta_t}{\sinh(q_a-\theta_t)\eta_t^+(q_a-\theta_t)},$$

$$\phi_{a2}=-\frac{\Delta+1}{2}\frac{\eta_t^-(q_a-\theta_t)}{\sinh(q_a-\theta_t)\eta_t^+(q_a-\theta_t)},$$

$$\phi_{a3}=\frac{1-\Delta}{2},$$

$$\phi_{b1} = \frac{\Delta+1}{2\Delta}\frac{\delta v_{yb}^0 \sinh\theta_r}{\sinh(q_b+\theta_r)\,\eta_t^-(q_b+\theta_r)},$$

$$\phi_{b2} = -\frac{\Delta+1}{2\Delta}\frac{\eta_r^+(q_b+\theta_r)}{\sinh(q_b+\theta_r)\,\eta_r^-(q_b+\theta_r)},$$

$$\phi_{b3} = \frac{\Delta-1}{2\Delta}.$$

We see that the sonic functions on the right-hand sides of Eqs. (60) and (61) are shifted, due to the Doppler shift at the shock fronts. This characteristic certainly complicates the mathematical procedure to get an analytically closed solution. Nevertheless, as has been shown in Ref. [9], we can always get the exact growth rate by means of an adequate iteration procedure which converges very fast.

4. Asymptotic perturbation velocities at the rippled contact surface

Our next task is to derive an expression for the asymptotic normal perturbed velocity at $x=0$. This can be done, noting that the time integral of the linearized tangential momentum equation from $t=0+$ up to $t=\infty$, at both sides of the interface, gives us

$$R(\delta v_{ya}^\infty - \delta v_{ya}^0) = (\delta v_{yb}^\infty - \delta v_{yb}^0), \tag{62}$$

where δv_{ym}^∞ is the asymptotic value of the tangential velocity at $x=0$. Furthermore, we also have the following relationships, as can be deduced from the definitions of the functions F from Eqs. (38) and (39) [9]:

$$\delta v_i^\infty = F_{m2}(q_m=0) - F_{m1}(q_m=0), \tag{63}$$

$$\delta v_{ym}^\infty - \delta v_{ym}^0 = F_{m2}(q_m=0) + F_{m1}(q_m=0), \tag{64}$$

where m can be either "a" or "b." We further define the following quantities:

$$F_a = \delta v_i^\infty + \delta v_{ya}^\infty, \tag{65}$$

$$F_b = -\delta v_i^\infty + \delta v_{yb}^\infty. \tag{66}$$

Thanks to Eqs. (46), (54), and (62)–(66), we get the expressions for the parameters F_a and F_b:

$$F_a = \left[1 + \frac{4(u_t - v_i)}{v_i}(1+\beta_t h_t)^{-1}\right]^{-1}[\delta v_{ya}^0 - 2F_{a1}(-2\theta_t)], \tag{67}$$

$$F_b = \left[1 + \frac{4(u_r + v_i)}{v_1 - v_i}(1+\beta_r h_r)^{-1}\right]^{-1}[\delta v_{yb}^0 - 2F_{b2}(2\theta_r)]. \tag{68}$$

Finally, adding and substracting δv_i^∞ in Eq. (62), we arrive after some simple manipulation to an expression for the growth rate at the interface, already presented in Eq. (5):

$$\delta v_i^\infty = \frac{\delta v_{yb}^0 - R\,\delta v_{ya}^0}{R+1} + \frac{RF_a - F_b}{R+1}. \tag{69}$$

It can be seen, according to Ref. [9], that the sonic parameters $F_{a,b}$ can be rewritten as averages of the vorticity profiles at both sides of the interface, as left by the corrugated fronts in the interior of the fluids. In fact, as has been seen in Refs. [6,7], the vorticity generated at either side of the interface can be formally written as

$$\delta\omega_b(x,y) = g_b(x)\sin ky = \Omega_b(\delta\hat{p}_r)_{t_0(x)=x/(u_r+v_i)}\sin ky, \tag{70}$$

$$\delta\omega_a(x,y) = g_a(x)\sin ky = \Omega_a(\delta\hat{p}_t)_{t_0(x)=x/(u_t-v_i)}\sin ky, \tag{71}$$

where the quantities $\Omega_{a,b}$ are

$$\Omega_a = -\frac{(1+\beta_t h_t)v_i}{2\beta_t(u_t - v_i)}, \tag{72}$$

$$\Omega_b = \frac{(1+\beta_r h_r)(v_1 - v_i)}{2\beta_r(u_r + v_i)}. \tag{73}$$

From the last equations, it is recognized that the vorticity is generated at x at the time $t=t_0(x)$ at which the shock arrives to that point. The continuity of tangential velocity across the corrugated front is responsible for generating the rotational part of the velocity field which makes up the vorticity field described in the above equations. After some additional algebra (explained in Refs. [7,9]), the sonic parameters F_a and F_b can be seen to be equal to the following spatial averages of the vorticity field:

$$F_a = -\Omega_a \sinh\theta_t \delta P_t(s_a = -\sinh\theta_t), \tag{74}$$

$$F_b = \Omega_b \sinh\theta_r \delta P_r(s_b = \sinh\theta_r). \tag{75}$$

Whatever representation we choose to deal with $F_{a,b}$, they have to be calculated with the aid of the functions $F_{m1,2}$ which describe the traveling pressure fluctuations. But to get them, we must solve the functional equation system of Eqs. (60) and (61). The details of the procedure to get the exact solution of those equations has been explained in Ref. [9] and will not be repeated here. We just remind that the process is an iteration sequence which gives us improved values of the sonic functions $F_{m1,2}$ with increasing accuracy. We only review the very basic steps. In fact, Eqs. (60) and (61) can be rewritten as

$$\mathbf{F} = R\Phi_0 + \mathbf{T}\mathbf{F}, \tag{76}$$

where $\mathbf{F}=(F_{a1}(q_a), F_{b2}(q_b))$, and the matrices $\mathbf{R}$ and $\mathbf{T}$ are given by

$$\mathbf{R} = \begin{pmatrix} -2(\Delta-1)/(\Delta+1)^2 & 4\Delta/(\Delta+1)^2 \\ 4\Delta/(\Delta+1)^2 & 2\Delta(\Delta-1)/(\Delta+1)^2 \end{pmatrix} \tag{77}$$

$$\mathbf{T} = \mathbf{R}\cdot\begin{pmatrix} \phi_{a2}e^{-2\theta_t D_a} & 0 \\ 0 & \phi_{b2}e^{2\theta_r D_b} \end{pmatrix}. \tag{78}$$

In the last matrix, the exponents are to be understood as traslation operators, that act on the functions to their right

evaluating them at a shifted value, that is: $e^{-2\theta_t D_a}[F_{a1}(q_a)] = F_{a1}(q_a - 2\theta_t)$, and similarly for the variable "b" (where $D_a = d/dq_a$). Equation (76) can be solved by iteration by a proper choice of the guess function. This is explained in some detail in Ref. [9]. We quote here the iteration chain:

$$\mathbf{F}^{[\mathbf{n}]} = \mathbf{\Xi_0} + \mathbf{T}\mathbf{F}^{[\mathbf{n-1}]}, \tag{79}$$

where $\mathbf{\Xi_0} = \mathbf{R}\mathbf{\Phi_0}$. The seed functions, with which we start the iteration, are given by [9]

$$F_{b2}^{[0]}(q_b) = \frac{\phi_{a1} - \phi_{b1}(\phi_{a3} - \phi_{a2})}{1 - (\phi_{b3} - \phi_{b2})(\phi_{a3} - \phi_{a2})}. \tag{80}$$

$$F_{a1}^{[0]} = \phi_{b1} - \phi_{b3}F_{b2}^{[0]}(q_b) + \phi_{b2}F_{b2}^{[0]}(q_b + 2\theta_r). \tag{81}$$

It has been shown that the iteration process defined by Eqs. (79)–(81) give very precise values for the functions $F_{m1,2}$, and hence, a highly accurate determination of the rate of growth δv_i^{∞} [9].

III. CALCULATION OF FREEZE-OUT CONDITIONS

In this section we calculate the points, in the space of pre-shock parameters, for which we can find asymptotic freeze-out of the normal ripple velocity. The idea is to set the value of Eq. (5) [or Eq. (69)] to zero and solve for the initial density jump by iteration. We rewrite the expression that gives the asymptotic normal velocity from Eq. (5), in the form:

$$\delta v_i^{\infty} = \delta v_{\text{irrot}} + \delta B \tag{82}$$

where

$$\delta v_{\text{irrot}} = \frac{\delta v_{yb}^0 - R\,\delta v_{ya}^0}{R+1} \tag{83}$$

is the irrotational contribution to the ripple asymptotic velocity and

$$\delta B = \frac{RF_a - F_b}{R+1} \tag{84}$$

is the contribution from the vorticity deposited in the interior of both fluids (or equivalently, it is the asymptotic effect of the sound wave reverberations that took place during the compressible phase: $0 < t < \infty$) [5,7,9]. The idea is to calculate δv_i^{∞} with a first guess for the density jump, which we choose: $R_0^{[0]} = 1$. With this initial guess value of R_0 we calculate the corresponding value of $\delta B^{[0]}$ according to the definitions of the previous section. The next step is to rewrite the equations that define the transmitted and reflected shock intensities [Eqs. (10) and (11)], but allowing now for R_0 to be another unknown. Therefore, Eq. (69) must be added as an additional equation, as we will have a new set of three unknowns: $z_r^{[1]}$, $z_t^{[1]}$, and $R_0^{[1]}$. Once we solve for them, we go again to Eq. (82) and calculate the new value of $\delta B^{[1]}$, using the iterated new value $R_0^{[1]}$. The new value of δB is used to calculate new values for the shock intensities and the density ratio, which in turn are used to calculate the following new value of δB and so on. The process does converge quite fast and we achieve enough digits of precision with few iteration steps. As the precision in the determination of R_0 increases, the value of δv_i^{∞} is decreased by many orders of magnitude after several iteration steps, approaching the condition for freeze-out: $\delta v_i^{\infty} = 0$.

We write here the nth iteration step. The system of equations that gives the shock intensities and the pre-shock density jump is

$$\frac{z_i}{\sqrt{1+\epsilon_{b1}z_i}} - z_r^{[n]}\sqrt{\frac{(1+z_i)}{(1+\epsilon_{b1}z_r^{[n]})}\frac{\rho_{b0}}{\rho_{b1}}} = \sqrt{\frac{\gamma_b}{\gamma_a R_0^{[n]}}}\frac{z_t^{[n]}}{\sqrt{1+\epsilon_{a1}}},$$

$$z_t^{[n]} = z_i + (1+z_i)z_r^{[n]},$$

$$\delta v_{\text{irrot}}^{[n]} = -\sigma B^{[n-1]}, \tag{85}$$

where $\delta B^{[n-1]}$ is calculated with

$$\delta B^{[n-1]} = \frac{R^{[n-1]}F_a^{[n-1]} - F_b^{[n-1]}}{R^{[n-1]}+1}. \tag{86}$$

In Fig. 5 we show slices of the function $R_0 = R_0(\gamma_a, \gamma_b, M_i)$, for which we should expect freeze-out. The value chosen for the isentropic exponent of the heavier fluid is $\gamma_a = 1.8$. That of the lighter fluid (γ_b) is varied between 1.1 and 1.7 and the incident shock Mach number (M_i) is varied between 1 and 5. In Fig. 6 we show the same function for $\gamma_a = 5/3$, with $1.05 \leqslant \gamma_b \leqslant 1.4$. We see that the values of the initial density ratio at which freeze-out is observed are very near $R_0 = 1$. We have not found freeze-out for larger values of R_0 [10,11]. This is certainly related to the fact evidenced in Sec. I: to be near freezing-out conditions, the transmitted shock speed should be higher than the incident shock velocity to allow for the tangential velocity on the heavier side to have the same sign as the tangential velocity on the lighter side. This seems to be only achievable for fluids of nearly equal densities, at least for the case in which a shock is reflected. We also see that, for the parameters range studied here, the density ratio at which freeze-out is expected, slightly increases as the incident shock Mach number increases and the lighter fluid becomes more compressible. We could not find freeze-out interchanging the values of γ at both sides of the interface. That is, the fluid in which the transmitted shock travels should have a larger isentropic exponent than the other fluid (the "incident" fluid). Otherwise, the speed of the transmitted front cannot be higher than the incident shock speed, and the circulation at the interface could not change the sign, a necessary condition for freeze-out as discussed before. In fact, if we interchange the values of γ (making $\gamma_a < \gamma_b$), we cannot have a reflected shock, because the density ratio is almost unity. That is, for $R_0 \sim 1$, Eq. (85) does not have a real solution for $\gamma_a < \gamma_b$ [3]. In the next section we discuss the results obtained and compare them with previously reported freeze-out situations.

IV. DISCUSSION

In this section we will discuss the results obtained with the method outlined in the previous paragraphs. It is shown,

based on the cases discussed in Sec. I, that we can get another useful picture of freeze-out. As mentioned in Sec. I, it turns out that freeze-out can be thought of as the result of an adequate balance between the tangential velocities generated at the contact surface, at $t=0+$. Accordingly, there should exist a critical value for the ratio $K_0=\delta v_{ya}^0/\delta v_{yb}^0$, such that, when K_0 reaches that specific value, freeze-out would be observed. For K_0 above or below such critical value, nonzero growth of either sign would occur. After showing this, the accuracy of a weak shock approximation to freeze-out is discussed. Finally, previously reported cases of freeze-out are studied with some detail.

A. Critical value of $\delta v_{ya}^0/\delta v_{yb}^0$

As we have seen in Sec. I, depending on the relative values of the transmitted and incident shock speeds, we can change the phase of the transmitted shock with respect to the pre-shock ripple at the interface. Above some minimum value of the ratio u_t/u_i, we would be able to see an indirect phase inversion of the interface ripple, as had been previously found in Ref. [3]. Therefore, for some specific value of u_t/u_i we could expect zero asymptotic growth. That this is actually feasible has been demonstrated in the previous sections and it has been shown that there is a continuum of values of the four dimensionless parameters at which this effect is possible. We could ideally think of the region of freezing-out as a hypersurface of the form: $R_0=R_0(\gamma_a,\gamma_b,M_i)$, as discussed in Ref. [3]. Unfortunately, it is not possible to show a simple closed formula that defines this hypersurface. Due to the complexity of the procedure followed to identify the freeze-out zones, it is not evident to foresee whether such a surface exhibits interesting topological features or not. For example, it could be possible that this surface showed kinks or folds, or that there could be even unconnected islands of freeze-out in the parameter space. In this work we have only found freeze-out regions that cluster around the $R_0\approx 1$ region. The only way to rule in/out the possibility of those fascinating properties, would be an exhaustive mapping of the whole parameter space using the algorithm presented in the previous section. This task is beyond the scope of the present work and is left for future research. Presented in this way, the reason for freeze-out seems to be hidden in a subtle and precise tuning of two zero-order speeds, which can be selected by proper choice of the four parameters of the problem. Once the exact point of freeze-out has been chosen, the asymptotic normal velocity vanishes for all perturbation wavelengths. That is, this is not a kind of selective stabilization which holds above certain threshold value for the wave number, as is usual in instabilities driven by gravity [Rayleigh-Taylor instability (RTI)], or shear velocity [Kelvin-Helmholtz instability (KHI)], and acted on by some other mechanism as surface tension or dissipative processes like viscosity, thermal conduction or ablation (as is commonly found in ICF environments) [5,17]. There is no dissipative physics here and the fluids in which the shocks are traveling are taken to be ideal gases. The only apparent mechanism that drives the surface ripple toward freezing-out is the "push and pull" effect, provided by the continuous influence of the pressure field radiated by the shock waves, which arrive with some delay to the interface. These waves refract there, altering the kinematics of the surface ripple, to arrive at the shock some time later, and repeat the process. Until the shocks are some wavelengths away from the contact interface, the contact surface ripple will oscillate in damped fashion to stop asymptotically.

We present here the conditions for freeze-out in a slightly different, but also convenient way. As discussed in Sec. I, there should be a relationship between δv_{ya}^0 and δv_{yb}^0 at the exact point of freeze-out. To stress this fact, we define the parameter:

$$K_0=\frac{\delta v_{ya}^0}{\delta v_{yb}^0}. \tag{87}$$

As we have seen in Sec. I, we need that both tangential velocities have the same sign. That is, we must have $K_0=K_0^{\mathrm{fo}}$ for some characteristic value $K_0^{\mathrm{fo}}>0$. For $K_0<K_0^{\mathrm{fo}}$ the growth of the ripple should be in the positive direction. For $K_0>K_0^{\mathrm{fo}}$, we should see an indirect phase inversion of the interface and hence, growth in the negative direction. Our task is to show that this is indeed the case.

After some lengthy algebra, we can rewrite the parameters $F_{a1}(-2\theta_t)$ and $F_{b2}(2\theta_r)$ in the following, more suitable form:

$$F_{a1}(-2\theta_t)=\sigma_{a1}\delta v_{ya}^0+\sigma_{b1}\delta v_{yb}^0,$$

$$F_{b2}(2\theta_r)=\sigma_{a2}\delta v_{ya}^0+\sigma_{b2}\delta v_{yb}^0, \tag{88}$$

where the quantities $\sigma_{a1,2}$ and $\sigma_{b1,2}$ can be obtained with an iterative process from Eqs. (79)–(81). The exact form of the recurrence relationships necessary to obtain the four quantities $\sigma_{a1,2}$, $\sigma_{b1,2}$ is not strictly necessary right now, in order to follow the qualitative discussion of this section. We should note, however, that instead of dealing with a functional equation for the functions F_{a1} and F_{b2}, we could express the bulk term δB [Eq. (84)] in terms of the σ quantities mentioned above. The interested reader could work out the corresponding new functional equations for $\sigma_{m1,2}$ without any big difficulties. As our interest here is only to reinterpret the physics behind the phenomenon of freeze-out, we will only work with Eq. (88) above. In fact, inserting the shock functions into the expression for the bulk vorticity term in Eq. (82), we arrive at

$$K_0=\frac{\delta v_{ya}^0}{\delta v_{yb}^0}=\frac{\frac{1}{R}\frac{Z_b-1}{Z_a-1}+\frac{2Z_a\sigma_{b1}}{Z_a-1}-\frac{2Z_b\sigma_{b2}}{R(Z_a-1)}}{1-\frac{2Z_a\sigma_{a1}}{Z_a-1}+\frac{2Z_b\sigma_{a2}}{R(Z_a-1)}}$$
$$+\left(\frac{R+1}{R}\right)\frac{\frac{\delta v_i^\infty}{\delta v_{yb}^0}}{(Z_a-1)\left[1-\frac{2Z_a\sigma_{a1}}{Z_a-1}+\frac{2Z_b\sigma_{a2}}{R(Z_a-1)}\right]}, \tag{89}$$

where the quantities $Z_{a,b}$ are taken from Eqs. (67) and (68):

$$Z_a = \left[1 + \frac{4(u_t - v_i)}{v_i} (1 + \beta_t h_t)^{-1} \right]^{-1},$$

$$Z_b = \left[1 + \frac{4(u_r + v_i)}{v_1 - v_i} (1 + \beta_r h_r)^{-1} \right]^{-1}. \quad (90)$$

Equation (89) above is the same as Eq. (69), and has the same information regarding instability growth at the material surface. However, some immediate, more apparent conclusions can be drawn from Eq. (89). At first, it is clear that, if we require $\delta v_i^{\infty} = 0$, the quantity K_0 should have a definite value K_0^{fo}, which is the first term on the right-hand side of Eq. (89). For $K_0 < K_0^{\mathrm{fo}}$, we would get positive growth and for $K_0 > K_0^{\mathrm{fo}}$, we would get negative values of the asymptotic growth. It is also clear that the condition $K_0 = K_0^{\mathrm{fo}}$ could be used instead of Eq. (69), as the equation used to find freeze-out. This would amount to changing the structure of the iteration process described in Eq. (85). The results of doing it are exactly the same as those obtained by solving Eq. (85) and therefore, nothing essentially new is gained, at least from the operational point of view. As a consequence, this strategy will not be used to re-derive the freezing-out conditions quantitatively, and the discussion will only remain at the qualitative level. The usefulness of presenting Eq. (89) is that it actually confirms our previous picture of freeze-out, as has been thoroughly discussed in Sec. I. That is, there should be enough vorticity on one side of the interface (the fluid with larger isentropic exponent) such that an indirect phase inversion is induced. However, at freeze-out, the phase inversion is never complete, because the interface stops growing some time later. If $\delta v_{ya}^0 / \delta v_{yb}^0$ has the correct value, the subsequent "push-pull" effect of the incoming sound waves will not be strong enough to force the interface growing in either direction, and hence the interface ripple would stop for large times. It will, perhaps, grow in the negative direction for a while and stop growing asymptotically. If the ratio K_0 has not the correct value, then depending on which side the tangential velocity is the largest, the incoming sound waves will induce growth toward the side privileged by the difference $K_0 - K_0^{\mathrm{fo}}$. It can be seen, after some long and tedious but not difficult algebra, that the quantities $Z_a \sigma_{a1}$ and $Z_b \sigma_{b2}$ are negligible for very weak shocks. Then, it is tempting to simplify the expression for K_0^{fo} above with just the first fraction in the numerator of the first term in Eq. (89). That is, we could define an approximate expression for the threshold value of K_0:

$$K_0^{\mathrm{approx}} \equiv \frac{1}{R} \frac{Z_b - 1}{Z_a - 1}. \quad (91)$$

In Fig. 7 we study the values of the exact quantity K_0^{fo} and its approximate estimation K_0^{approx} for the cases $\gamma_a = 1.8$ and $1.1 \leqslant \gamma_b \leqslant 1.7$ for $1 \leqslant M_i \leqslant 5$, as used in Fig. 5. The solid line is the exact value for the velocity ratio [Eq. (89)] and the dashed lines are the values given by the approximate expression [Eq. (91)]. We see that except at very high compressions, the approximate expression does a good job in predicting the critical velocity ratio at freeze-out. An obvious conclusion from the results shown in Fig. 7 is the fact that $\delta v_{ya}^0 > \delta v_{yb}^0$ seems to be a necessary condition for freeze-out.

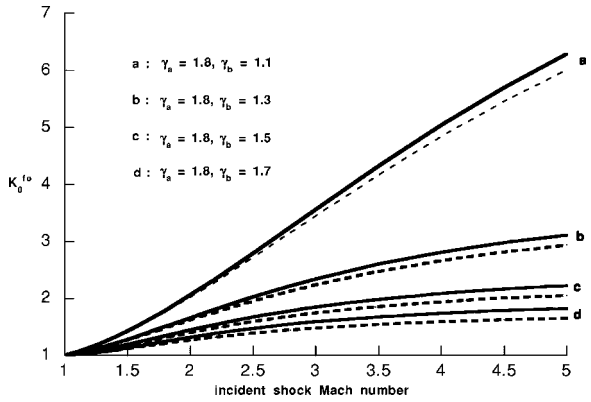

FIG. 7. Curves (solid) of the parameter K_0^{fo} in freeze-out [Eq. (89)], as a function of the incident Mach number (M_i), for the parameters shown. The dashed lines are calculated with the approximate value K_0^{approx}, as discussed in Eq. (92).

B. Weak shock approximation in the search of freeze-out

When we look at Eq. (82) we see that the rate of growth at the interface is composed by two terms: an irrotational contribution ($\delta v_{\mathrm{irrot}}$), and a bulk contribution which expresses the fact that there is vorticity continuously distributed at both sides of the interface [5–10,12]. This vorticity field is the memory of the previously corrugated shock fronts that emitted sound pressure perturbations and generated stationary profiles of vorticity and entropy fluctuations along their way. Making the bulk term in each side of the interface strictly equal to zero ($\delta B = 0$) would be actually equivalent to ignoring the role of the corrugated shock waves after $t = 0+$ or to assuming that the fronts that separated away from the interface were of an isentropic nature. This last possibility could be certainly the case if those fronts were rarefaction fans expanding away from the contact surface, as discussed by Velikovich [4]. Indeed, his symmetrical Riemann problem for the rarefactions escaping away would actually perfectly fit this idealized situation, because in this case it would be $F_a = F_b = 0$ exactly, and not merely as an approximation. In the rarefaction reflected RM instability we find, in fact, a situation in which one of the bulk parameters is exactly zero: the one pertaining to the expanding fluid, between the contact surface and the rarefaction trailing edge [4,5,18]. However, inside the fluid compressed by the transmitted shock we would still have the parameter $F_a \neq 0$. This is consequence of the fact that rarefaction fans are isentropic and hence entropy/vorticity preserving, while corrugated shocks are not. The conclusion is apparent: whenever we have a nonisentropic corrugated front which escapes away from the interface, we must expect entropy and vorticity perturbations which will affect the asymptotic growth at the interface at a later time. These vorticity fluctuations cannot arrive at the interface, as they are frozen to the fluid elements at the position where that vorticity has been created. Therefore, the contact surface ripple has no way "to know" about them immediately and adjust its circulation to the evolving veloc-

ity field in the bulk. The only way to adjust the velocity values at both sides of the interface and make them compatible with the vorticity field on each fluid is by means of the sound waves emitted by the fronts in the interval of time $0<t<\infty$. Therefore, there is no contradiction in the "dual" interpretation we have assigned to the parameters F_a and F_b. They can be seen as the dynamical effect of the sound waves pressure field during the period $0+\leqslant t<\infty$, and also as the asymptotic manifestation of that interaction in the form of a vorticity field at both sides of the interface for $t\rightarrow\infty$. The space integral of such vorticity field [for example, either Eq. (74) or (75)] has the correct value to ensure that the final asymptotic velocity field has consistently evolved from the initial circulation deposited at the interface to its final value. It is clear that the values of $\delta\Gamma_0$ and $\delta\Gamma_\infty$ must be consistent with any vorticity/velocity perturbation field in the bulk, as is clearly required by Eqs. (65), (66), (74), and (75). The only way to make the smooth transition from that initial circulation $\delta\Gamma_0=\delta v_{yb}^0-\delta v_{ya}^0$ to the corresponding asymptotic growth δv_i^∞ is to allow for the action of the early sound waves, which baroclinically would change the velocities at the contact surface. But these waves must come from somewhere ahead of the contact surface. In fact, that job can be done either with a pair of shocks or a pair of rarefaction fans, or with a shock and a rarefaction [4,5,7,9]. In the double rarefaction case (that is, the symmetrical Riemann problem discussed in Ref. [4]), the sound waves just alter the initial circulation $\delta\Gamma_0$, transforming it to its asymptotic value $\delta\Gamma_\infty$, without generating any vorticity in the bulk ($F_a=F_b=0$). The final velocity field will be, in this case, exactly irrotational. On the other hand, in the shock case (or in the case of having only one rarefaction reflected), the sound waves that arrive to the interface, alter the the initial circulation at the interface and bring it to its final value in a way that is consistent with the conditions expressed mathematically in Eqs. (65)–(68), (74), and (75). As we know from previous work [7,9], these conditions are necessary requirements that must be fulfilled to ensure the boundedness of the asymptotic velocity fluctuations very far from the contact surface (that is, at $|x|\rightarrow\infty$). As we are concentrating here on the shock case, we leave the rarefaction reflected situation for future work. A natural question to be asked is then: is it possible to deal with another more simple equation that defines freeze-out, which does not need to deal with the functional equations system defined in Eqs. (79)–(81)? That is, a simplified expression which can neglect the bulk vorticity term, in some range of the physical variables that define the problem? According to our knowledge, this can be done exactly, just by requiring the vanishing of δv_{irrot} in those cases in which we have no shocks. But this is not the case discussed here. However, as can be seen from simple inspection in Eqs. (72) and (73), the bulk vorticity parameters $\Omega_{a,b}$, are quantities of second order in the shock intensity z_i for very weak shocks [7,9]. This means that we could roughly neglect the term δB in Eq. (82), as a first approximation, and compare the approximate results with the exact procedure described before. That is, we look for the set of points in the space of initial parameters, for which the following equation holds, together with the conditions to have a reflected shock [Eqs. (10) and (11)]:

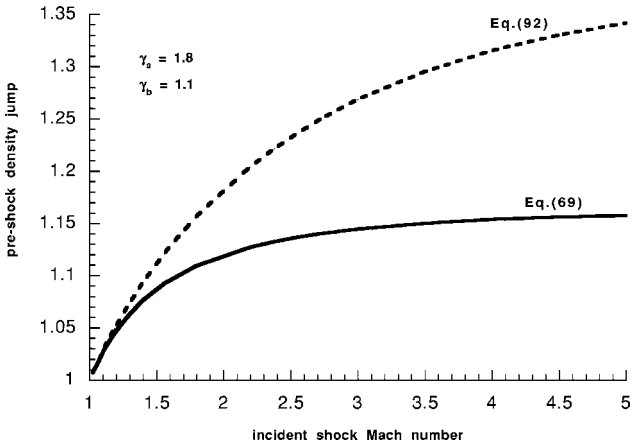

FIG. 8. Comparison of the curves predicted for freeze-out with the complete Eq. (69) and the irrotational approximation given by Eq. (92).

$$\delta v_{\text{irrot}}=\frac{\delta v_{yb}^0-R\,\delta v_{ya}^0}{R+1}=0. \tag{92}$$

It must be stressed that Eq. (92) has no information of the bulk vorticity, or in other words, no information of the shock-interface interaction through the multiple reverberations, giving us limited physical information of the instability evolution when vorticity production could be important (compressible fluids and/or strong shocks). Using Eq. (92) beyond its reduced limit of validity is certainly not justified by accidental or coincidental partial agreements with the exact solution at any higher shock intensities. In Fig. 8 we show the results deduced from the last equation, for a particular case: $\gamma_a=1.8$ and $\gamma_b=1.1$. The incident shock Mach number is varied in the interval $1\leqslant M_i\leqslant 5$. We also show the corresponding curve calculated exactly with the bulk contribution [Eqs. (85) and (86)]. The agreement is reasonably good for quite low compressions but it worsens for moderate to strong shocks. In Fig. 9 we show the actual growth veloc-

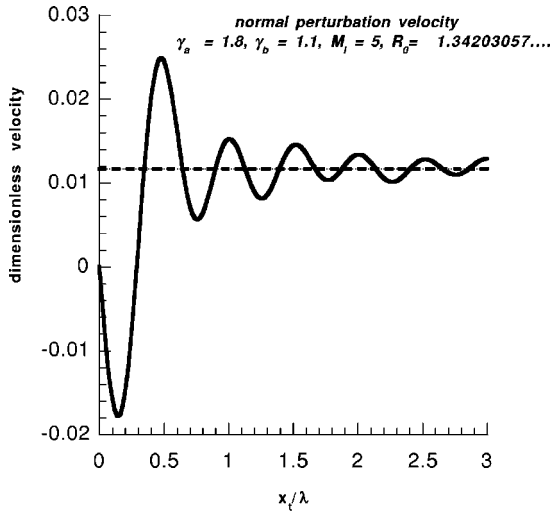

FIG. 9. Exact temporal evolution and asymptotic value for the normal velocity for the parameters shown.

ity at the contact ripple for $M_i=5$ and $R_0\approx 1.342\,030\,57\ldots$ for which freeze-out would be expected according to Eq. (92). Despite the fact that the asymptotic value is low ($\delta v_i^{\infty}\sim 0.012\, u_i k\psi_0$), it is however, not zero, and would lead to permanent deformation of the interface.

C. Comparison with previously predicted cases of freeze-out

The freeze-out problem has been attacked several times in the recent past as evidenced in the literature. Fraley was the first to mention, to our knowledge, the possibility of having zero growth for values $R_0<1.5$ in the shock reflected case [3–11]. Mikaelian [11] has studied for the first time this problem with some detail in the weak shock limit, using the model previously developed by Fraley [10]. Mikaelian reobtained the closed analytical expression given by Fraley for the growth rate, and derived a freeze-out condition for weak compressions and $R_0=1$. The conclusions of Mikaelian have been later reviewed by Brouillette [19]. The approximate growth rate, as obtained by Mikaelian, can be rewritten in our notation as

$$\delta v_i^{\mathrm{Mik}} = v_i k\psi_0\left(A_{T0}+\frac{z_i}{z_i+1}\frac{J}{\gamma_b}\right), \tag{93}$$

where $A_{T0}=(R_0-1)/(R_0+1)$ is the pre-shock Atwood number, and J is a quantity defined by

$$J=\frac{1}{2}\left[(w-1)^2-R_0-2w+\frac{2}{w}\left(\frac{(1+A_{T0})^2}{1-A_{T0}}+(1-A_{T0})w^2\right)\times\left(\frac{1-T_{T0}}{w+1}\right)\right], \tag{94}$$

and $w=\sqrt{R_0\gamma_a/\gamma_b}$. This last expression for the growth rate is valid in the limit: $z_i\ll 1$. It contains terms up to second order in z_i and therefore, it does contain some of the information carried by the bulk vorticity term δB. Hence, its predictions should be more accurate for low intensity shocks than the predictions of Eq. (92) are. It is easy to see, as discussed in Ref. [11], that for fluids with equal pre-shock densities ($R_0=1$), the above expression for the growth rate vanishes exactly if $\gamma_a=4\gamma_b$. This finding confirms our conclusion, derived earlier, that the fluid in which the transmitted shock travels should have a larger isentropic exponent than the other fluid. In Fig. 10, we compare Eqs. (82), (83), and (93) for the case $\gamma_a=4.4$, $\gamma_b=1.1$ for $R_0=1$ for incident shock Mach numbers between $1\leqslant M_i\leqslant 1.7$. We show the actual growth rate calculated with the exact formula given by Eq. (82), which is indicated with the solid line. The growth predicted by the irrotational assumption is shown with the dashed line [Eq. (83)]. The growth predicted by Mikaelian with Eq. (93) would be a perfectly horizontal line (zero growth) starting at the point $M_i=1$ (not shown). As suspected, the two conditions $R_0=1$ and $\gamma_a=4\gamma_b$ do not give exact freeze-out of the normal velocity at any intensity $z_i\ll 1$, except at $M_i=1$. However, the growth rate keeps very low ($\delta v_i^{\infty}<10^{-4}\, k u_i\psi_0$) until incident Mach numbers of the order of $M_i\sim 1.2$. With the aid of Eqs. (85) and (86) it can be seen that there is real freeze-out at $M_i\approx 1.623\,56\ldots$. The velocity values in the vertical axis have been indicated with a logarithmic scale to accurately emphasize the large range

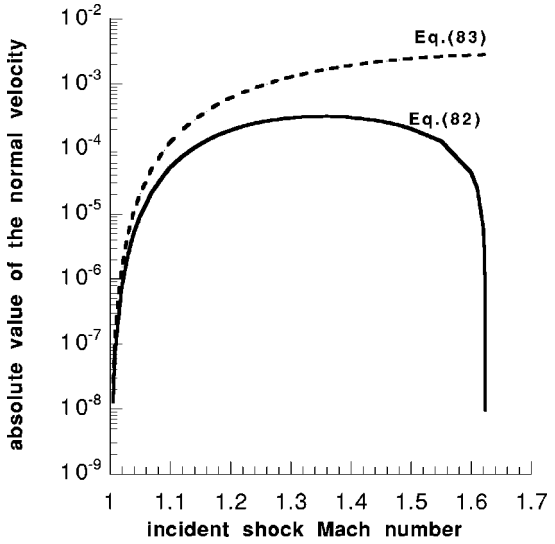

FIG. 10. Exact asymptotic normal velocity [solid curve, Eq. (82)] for the case $\gamma_a=4.4$, $\gamma_b=1.1$ in the weak shock limit. The dashed curve has been calculated with the irrotational approximation given by Eq. (83).

of variation as a function of the incident shock intensity. As commented before, the steep gradient of δv_i^{∞} as a function of M_i which occurs near the freeze-out point ($M_i\approx 1.623\,56\ldots$) could be indicating to us the possibility of a rich topological structure for the freeze-out hypersurface. In particular, this hypersurface could be even double-valued or exhibit disconnected regions or islands of freeze-out far away from the zone $R_0\sim 1$. Right now, the development of a simpler mathematical picture of that surface does not seem an easy task. An accurate mapping of this surface searching for those mathematical characteristics in the whole space of initial parameters would certainly be interesting and is left for future work.

Soon after the prediction of Mikaelian, the numerical solution to the linear RM instability problem by Yang, Zhang, and Sharp [3] tried to identify freeze-out for the case $\gamma_a=4.4$, $\gamma_b=1.1$. The authors solved the same equations as here with an improved numerical technique as used by Richtmyer, and obtained the temporal evolution of the two important cases in the RM instability, whether a shock or a rarefaction are reflected. To compare with their findings, we have found that, for the values $\gamma_a=4.4$, $\gamma_b=1.1$, and $M_i=1.28$, freeze out is expected at $R_0=1.002\,626\,158\,2\ldots$. In Fig. 11(a) we show the interface tangential velocity of fluid "*a*" as a function of time. The analogous quantity for fluid "*b*" is shown in Fig. 11(b). As can be seen, either the initial or final circulations at the interface are negative, in agreement with the qualitative picture discussed in the previous paragraphs. The asymptotic values are: $\delta v_{ya}^{\infty}\approx 0.003\,524\, u_i k\psi_0$ and $\delta v_{yb}^{\infty}\approx 0.000\,865\,0\, u_i k\psi_0$. It is noted a more or less general characteristic of freeze-out: it is always seen that F_b is lower than F_a by at least an order of magnitude. This could be attributed to the relative "weakness" of the reflected shock compared to the transmitted front. In Fig. 11(c) we show the contact surface perturbation velocity as a function of time. The horizontal axis is the dimensionless time defined by: $\tau_i=k u_i t$. The

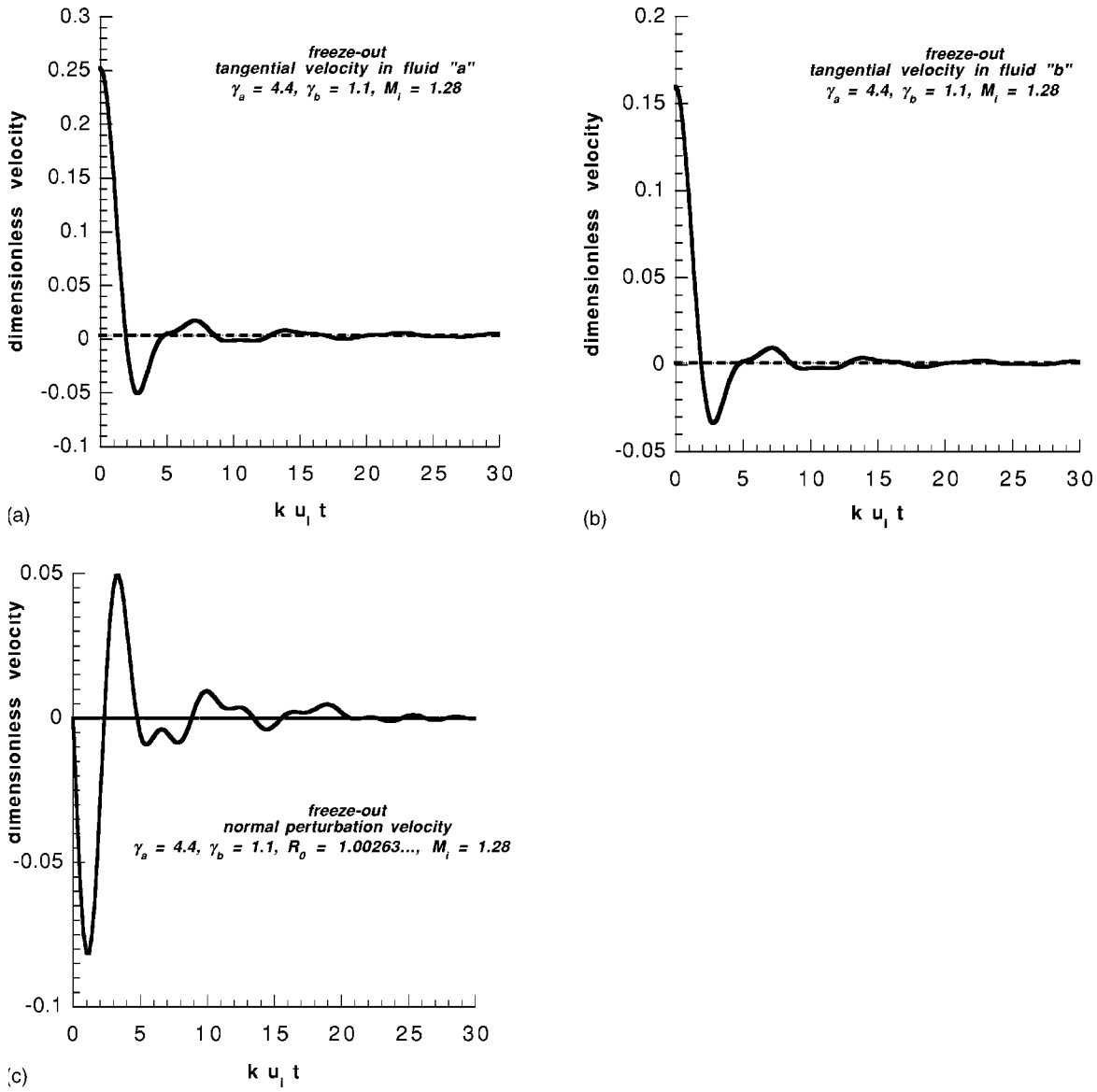

FIG. 11. (a) Freeze-out case, studied in Refs. [3,10]. Tangential velocity on fluid "*a*." (b) Same as (a), for the tangential velocity on fluid "*b*." (c) Same as (a), for the normal velocity at the contact surface.

agreement with Fig. 19 of Ref. [3] is indeed very good.

As a final comment about the perturbation field in freeze-out, we stress out again that despite the fact that the asymptotic normal growth would be negligibly small near the interface in freeze-out, there still could be considerable motion in the bulk of the fluids, essentially due to the vorticity that has been generated by the deformed fronts. Those vorticity fields are responsible for the jump in the tangential velocity at the interface, generating an asymptotic circulation $\delta\Gamma_\infty = \delta v_{yb}^\infty - \delta v_{ya}^\infty$. Therefore, there is some kinetic energy trapped inside the vortical motion in the bulk which is never zero. Its effect would be that of perturbing even further any subsequent shock launched toward the interface, despite the interface being asymptotically quiescent. Only in the case in which the bulk parameters (F_a and F_b) are strictly zero, we would have no velocity perturbations. However, this situation is not possible when there are two shocks separating away from the interface. The task of computing the kinetic energy that remains as rotational motion is beyond the scope of this work and is also left for future research.

V. CONCLUSIONS

We have presented an analytic work to study the conditions under which freeze-out of the Richtmyer-Meshkov could be expected for the shock reflected case. Based on previous analytical works, the mathematical conditions for freezing-out are derived. It is seen that those conditions are equivalent to asking for a given critical relationship between the initial tangential velocities at the contact surface ripple, as generated by the corrugated wave fronts. The role of the sonic reverberating pressure waves between the interface and the shocks is discussed, as is also emphasized the role of the vorticity field left by the shock fronts at each side of the

contact surface. An analytical procedure to derive the precise location in the space of physical parameters has been shown. An approximate equation only valid in the very weak shock limit is also discussed. A similar approximation discussed in the recent literature is also compared to our results. Previous numerical findings are seen to agree quite well with the results presented here.

ACKNOWLEDGMENTS

J.G.W. wishes to acknowledge kind hospitality and support of the ILE at Osaka University. Part of this work also received support from the Ministry of Education y Ciencia, Spain, FTN2003–00721.

[1] R. D. Richtmyer, Commun. Pure Appl. Math. **13**, 297 (1960).
[2] E. E. Meshkov, Fluid Dyn. **4**, 101 (1969).
[3] Y. Yang, Q. Zhang, and D. H. Sharp, Phys. Fluids **6**, 1856 (1994).
[4] A. L. Velikovich, Phys. Fluids **8**, 1666 (1996).
[5] A. L. Velikovich, J. P. Dahlburg, A. J. Schmitt, J. H. Gardner, L. P. Phillips, F. L. Cochran, Y. K. Chong, G. Dimonte, and N. Metzler, Phys. Plasmas **7**, 1662 (2000).
[6] J. G. Wouchuk and K. Nishihara, Phys. Plasmas **3**, 3761 (1996).
[7] J. G. Wouchuk and K. Nishihara, Phys. Plasmas **4**, 1028 (1997).
[8] N. J. Zabusky, Annu. Rev. Fluid Mech. **31**, 495 (1999).
[9] J. G. Wouchuk, Phys. Rev. E **63**, 056303 (2001).
[10] G. Fraley, Phys. Fluids **29**, 376 (1986).
[11] K. O. Mikaelian, Phys. Fluids **6**, 356 (1994).
[12] N. J. Zabusky, A. D. Kotelnikov, Y. Gulak, and G. Peng, J. Fluid Mech. **475**, 147 (2003).
[13] L. D. Landau and E. M. Lifshitz, *Fluid Mechanics*, 2nd ed. (Butterworth-Heinemann, Oxford, 2000).
[14] Ya. B. Zeldovich and Yu. P. Raizer, *Physics of Shock Waves and High-temperature Hydrodynamic Phenomena* (Dover, New York, 2002).
[15] G. B. Whitham, *Linear and Nonlinear Waves* (Wiley, New York, 1974).
[16] R. M. Zaidel', J. Appl. Math. Mech. **24**, 316 (1958).
[17] S. Chandrasekar, *Hydrodynamic and Hydromagnetic Stability* (Dover, New York, 1981).
[18] J. G. Wouchuk, Phys. Plasmas **8**, 2890 (2001).
[19] M. Brouillette, Annu. Rev. Fluid Mech. **34**, 445 (2002).